NLOS MITIGATION FOR ULTRA WIDEBAND LOCALIZATION

BY

KHALED MESFER ALQAHTANI

A Thesis Presented to the

DEANSHIP OF GRADUATE STUDIES

KING FAHD UNIVERSITY OF PETROLEUM & MINERALS

DHAHRAN, SAUDI ARABIA

In Partial Fulfillment of the

Requirements for the Degree of

MASTER OF SCIENCE

In

TELECOMMUNICATION ENGINEERING

Dec 2011

Scanned by CamScanner

KING FAHD UNIVERSITY OF PETROLEUM AND MINERALS

DHAHRAN 31261, SAUDI ARABIA

DEANSHIP OF GRADUATE STUDIES

This thesis, written by **Khaled Mesfer AlQahtani** under the direction of his thesis advisor and approved by his thesis committee, has been presented to and accepted by the Dean of Graduate Studies, in partial fulfillment of the requirements for the degree of **MASTER OF SCIENCE IN TELECOMMUNICATION ENGINEERING.**

Thesis Committee

9/4/2012

Dr. Ali Muqaibel (Advisor)

9/4/2012

Dr. Abdallah Al-Ahmari (Co-advisor)

9/4/2012

Dr. Mohamed Adnan Landolsi (Member)

Dr. Wessam Mesbah (Member)

9/4/12

Dr. Maan Kousa (Member)

Dr. Ali Al-Shaikhi

Department Chairman

Dr. Salam A. Zummo
Dean of Graduate Studies

Date 23/4/12

Scanned by CamScanner

DEDECATION

Dedicated to

My beloved Parents

ACKNOWLEDGEMENTS

All praise is to Allah (SWT), Lord of the Heavens and the Earths, and what they contain; most Beneficial, Most Merciful. I seek His benediction on our beloved Prophet, the best of humankind, Muhammad (SAW), his household and his companions, until the Day of Judgment. I thank Allah for His infinite bounties on me, one of which is the completion of this work; I seek His mercy and forgiveness, and indeed, I fear His wrath.

My gratitude, without reservation, goes to my parents for their endless support and prayers throughout my life. I will forever remain grateful.

I would like to convey my sincere gratitude to my thesis advisor Dr. Ali Hussein Muqaibel for his support and guidance. I thank him for being available whenever I needed his assistance. It is my pleasure working with him. I would like also to thank coadivsor Dr. Abdallah AlAhmari for his endless help and support. It is my pleasure working with him.

Special thanks to distinguished members of my thesis committee Dr. Adnan Al-Andalusi, Dr. Maan Kousa and Dr. Wessam Mesbah; first, for accepting to be on my thesis committee, further, for their useful guidance, motivation, and professional contribution to my success and that of this work.

I acknowledge the contribution of Mr. Umar M. Johar who was instrumental in carrying out the experimental part of this work. I also extend my appreciation to the UWB High Resolution Positioning group for their support and motivation.

I acknowledge my brothers and sisters for their support; my wife for her emotional support; my friends for their best wishes and help; and KFUPM, for the opportunity it gave me to study and accomplish this work. To all, I remain grateful.

TABLE OF CONTENTS

Contents

LIST OF TABLES

LIST OF FIGURES

THESIS ABSTRACT (ENGLISH)

NAME: Khaled Mesfer AlQahtani

TITLE: NLOS Mitigation for Ultra Wideband Localization

MAJOR: TELECOMMUNICATION ENGINEERING

DATE: DECEMBER 2011

One of the interesting properties of ultra wideband (UWB) signal is its superior performance and high accuracy in localization applications. This is due to its high resolution resulting from its small pulse duration that is in the order of nanoseconds. However, this accuracy is affected by several factors and among those factors is the non line of sight (NLOS) propagation. In this work, we suggested an improved Residual weighting (Rwgh) mitigation algorithm to minimize the effect of NLOS. The work considers a UWB channel based on IEEE 802.15.4a channel model. Indoor and outdoor environments are both considered in the simulation. The localization part of the work is based on the approximate maximum likelihood time difference of arrival (AML-TDOA) algorithm as a localization algorithm. The simulation result shows an acceptable improvement in the localization accuracy. The work also includes the installation and implementation of a real time localization system provided by Ubisense. The work involves also the error evaluation of the system with different experimental scenarios in the lab. NLOS scenarios are also studied in this real time system.

MASTER OF SCIENCE DEGREE
KING FAHD UNIVERSITY OF PETROLEUM and MINERALS
Dhahran, Saudi Arabia

THESIS ABSTRACT (ARABIC)

الاسم: خالد مسفر القحطاني

العنوان: تخفيف غير خط البصرعن الترا الاتساع التعريب

التخصص: هندسة الاتصالات

التاريخ: ديسمبر 2011

واحدة من الخصائص المثيرة للاهتمام جدا النطاق العريض (UWB) إشارة غير أدائها المتفوق ودقة عالية في تطبيقات التعريب. ويرجع ذلك إلى ارتفاع قرارها الناتجة عن مدته نبض الصغيرة التي هي في ترتيب نانو ثانية هذا. ومع ذلك، تتأثر هذه الدقة من قبل العديد من العوامل وبين تلك العوامل هو خط غير البصر (NLOS) الانتشار. في هذا العمل، اقترحنا محسنة خوارزمية تخفيف الوزن المتبقية (Rwgh) للحد من تأثير NLOS. ويعتبر عمل قناة UWB على أساس IEEE نموذج القناة a802.15.4. تعتبر البيئات الداخلية والخارجية على حد سواء في المحاكاة. ويستند الجزء توطين العمل على الحد الأقصى لاختلاف الوقت التقريبي احتمال وصول (AML-TDOA) الخوارزمية كما خوارزمية الترجمة. نتيجة محاكاة تظهر تحسنا مقبولا في دقة الترجمة. ويشمل العمل أيضا على تركيب وتنفيذ نظام توطين في الوقت الحقيقي التي تقدمها Ubisense. ويشمل العمل أيضا تقييم الخطأ من النظام مع سيناريوهات تجريبية مختلفة في المختبر. تدرس سيناريوهات NLOS أيضا في هذا النظام في الوقت الحقيقي.

درجة الماجستير في العلوم

جامعة الملك فهد للبترول و المعادن

الظهران المملكة العربية السعودية

CHAPTER 1 INTRODUCTION

1.1 Overview

Mobile computing has evolved over the last several years and aimed to provide an access to the location of the mobile users anytime and anywhere. Knowledge of the users' location would help significantly in mobile networks planning; load balancing, handover algorithms, radio resources management, and other performance enhancement methods. Localization is also receiving increased importance in the public safety issues. This importance increases in the case of indoor safety issues where the outdoor localization techniques (GPS as an example) would fail to locate the target precisely. The alternative is the use of indoor localization techniques like Wi-Fi (802), Bluetooth or RFID but the obtained accuracy is limited.

Ultra wideband is an excellent candidate that would provide very high and robust localization capabilities. The accuracy of UWB localization is within few centimeters, which enables accurate tracking. In addition, UWB introduces low power consumption (mille-watts of power) and low cost in the design of the transceivers. For all the mentioned characteristics, UWB has been the focus of the research and development recently. It offers several applications such as wireless Universal Serial Bus (USB), see-through-the-wall radar, medical imaging, security applications, search-and-rescue, and control of home appliances, which led UWB to be the first candidate for home network.

Wireless localization techniques (UWB based and others) are affected by several sources of errors such as multipath propagation, resulting in fading, or multiple access interference. In addition to the mentioned sources, the non-line of sight (NLOS) propagation that occurs when there is no direct path between the mobile station (MS) and the base station (BS) affects wireless localization techniques severely. NLOS introduces a positive bias to the range measurement. Therefore, there is a great need to develop algorithms to mitigate the effect of NLOS in order to get a better range measurement. The mitigation of NLOS errors in UWB localization is the subject of this thesis.

1.2 Literature Review

This section summarizes the different directions of research proposed to mitigate NLOS error in time-based localization. This topic receives a considerable attention by researchers because NLOS error introduces the largest bias to the range measurement and that would severely degrade the localization accuracy. In addition, by considering indoor localization, NLOS error will typically exist, as the indoor environments are full of obstacles, walls and other objects that will obstruct the LOS path.

In the literature, the proposed methods of NLOS error mitigation can be classified into direct path (LOS path) detection and statistics-based detection. In the direct path approach, the research is concentrated on finding the direct path of the received multipath signal instead of picking the strongest value of the correlator output that may not be the direct path. On the other hand, in statistics-based detection approach, various types of statistical methods are used to mitigate the NLOS error. Those methods includes, Least

Squares (LS), Taylor Series (TS), Weighted Least Squares (WLS), filtering, and linear programming [Cas06], [Che99], [Caf98].

Starting with the first path estimation-based methods, Heidari et al [Hei07] classified the received channel profile into two main classes, detected direct path (DDP) and undetected direct path (UDP). The DDP condition occurs when the DP is detectable, which results in small ranging error. The UDP condition, however, occurs when the receiver is not able to detect DP and that will result in ranging errors. In [Hei07], a peak detection algorithm is applied to detect the first path. Assuming the channel is identified as NLOS and by knowing the statistics of the NLOS error given by [Ala06a], they subtract the error statistics from the TOA of the first detected path.

The statistical-based method which is our choice, on the other hand, are widely used by researchers as they rely on post-processing of the received signal and gives better results. In [Che99], Chen developed an algorithm to mitigate the NLOS errors by residual weighting (Rwgh) without the need to identify the NLOS range measurements. First, the measurements are divided into groups with each group containing at least three measurements to be able to find the 2D node location. After applying the Least Square (LS) estimator, a group of *intermediate node location* is obtained. The final Rwgh location estimate of the linear combination of the *intermediate node location* weighted inversely to their normalized residual. By doing so, Rwgh automatically suppress NLOS measurements in the final location estimate and thereby achieves the goal of NLOS mitigation. Of course, this proposed algorithm is computational demanding especially in the case of having a large set of reference nodes. Jiao et al [Jia07] proposed an extension to this work. They were trying to reduce the complexity of Chen [Che99] algorithm to

make suitable for sensors network application were the sensors have limited resources and a large number of reference sensors are available. After calculating the normalized residual of intermediate nodes locations, they chose the combination with the minimum normalized residual, and they set the number of reference nodes equal to the number of measurements inside of chosen combination. In [Che99] the algorithm with nine reference nodes calculates LS estimation 446 times while the algorithm in [Jia07] calculates only 40 times.

Assuming that the NLOS measurements have been identified, Kegen et al [Yu07] proposed Taylor-series based weighted LS algorithm and derived an optimal estimator when the measurement noise is Gaussian and the NLOS error is Rayleigh distributed.

Venkatesh et al [Ven07] presented a novel computationally efficient linear programming approach that effectively includes both LOS and NLOS range information in the estimation of the node location. Instead of discarding the NLOS reference nodes; they included them in order to enhance the localization accuracy.

Guvenc et al. [Guv07] used several statistical techniques, kurtosis RMS delay, to identify the channel. After that, they analyzed several WLS localization techniques such as identify and discard, soft weight selection and hard weight selection.

Chan et al [Cha06a] proposed a residual test (RT) algorithm where they first identify the LOS reference nodes and localize only using them. The identification principle is that when all measurements are LOS, the normalized residuals have central Chi-Square distribution. However, in the presence of NLOS the normalized residuals will have noncentral Chi-Square distribution.

Li et al. [Li06] approached NLOS error mitigation in two steps. In the first steps, they averaged the received signal over multiple frames to remove the zero mean AWGN noise. Then a rough TOA is obtained by detecting the peak of the correlated signal. Secondly, the two cross-correlations between the time-averaged waveform and the early-late gate signals are computed. Then error signal can be obtained by using the difference of these two cross-correlation signals. After that, they found TOA of the first path by detecting the first minimum square of the error signal.

The above NLOS mitigation work was not specifically done for UWB systems. Some of the concurrent work of NLOS mitigation in the UWB case was recently published, the work by [Mar10] performed an extensive indoor measurement with FCC-complaints UWB radios to quantify the effect of NLOS propagation. From the measured channel pulse responses, they obtained features to classify whether the received signal is NLOS or LOS one using a support vector machine (SVM) classifier. After that, they develop a SVM algorithm to mitigate NLOS without the need for statistical modeling of the channel.

[Xu11] derived a closed form expression of CLRB for TDOA UWB localization for both LOS and NLOS environments. In addition, they studied how the number of reference nodes and the geometry of the network affect the localization accuracy of the blind nodes. They found that the area within the reference nodes has less error.

In [End11], the authors proposed an iterative NLOS mitigation algorithm for medical application that uses NLOS compensation to correct for the NLOS bias.

The work in [Kan11] proposes a pre-processing algorithm that uses previous data of TDOA to mitigate errors caused by NLOS in real time location system RTLS. They also employed a Kalman filtering to alleviate the multipath error.

In [Sha07], from the characteristic of the NLOS error, the authors derived a mitigation algorithm from the signal propagation pathloss model. They also derived a modified expression taking care of the antenna direction. As for the implementation of the method, they propose a low complexity DP and Multipath Channel Profile (MCP) detection algorithms, which makes the method proper for practical application.

When modeling NLOS is considered, different NLOS error models are available in the literature. In [Hei09] and [Ala06b], a work that relates the bandwidth dependency to the UWB ranging error was introduced. However, the work was investigated for frequencies below 3 GHz. The effect of bandwidth on UWB ranging error was studied in [Cho07] for a 7 GHz bandwidth. In [Ira06] and [Gen06], an investigation of the error was discussed but without any modeling. An error modeling was introduced in the work presented in [Ala06a] but for a specific frequency, 6 GHz. In [Bel08], a model that includes both the distance and a wide range of bandwidth was proposed. Figure 1-1 below summarizes the available work in the literature.

One of our tasks is to select and implement a promising NLOS mitigation technique to UWB localization systems. Chen [Che99] algorithm is chosen for the mitigation part of this thesis, as it does not require any prior statistical knowledge about the NLOS channel. It only has a requirement on the minimum needed reference nodes to locate the target.

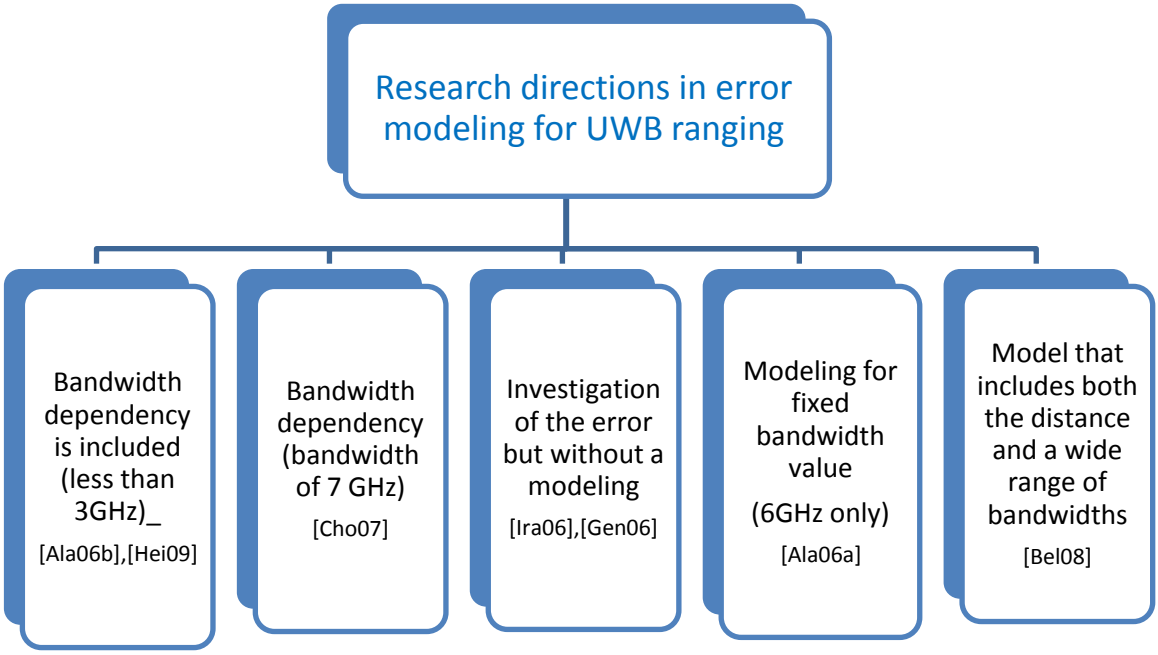

Figure 1-1: A summary of the research in modeling NLOS error in UWB

1.3 Thesis Contribution

The objective of this thesis work is to investigate localization for the promising UWB technology. Emphasis is given to NLOS propagation and possible mitigation techniques. To achieve the objective both experimental and simulation work are performed.

In the experimental part, we investigate a realistic UWB channel localization system. We implement, test and analyze the accuracy of the UWB Real Time Location System (RTLS) by Ubisense® in indoor environment.

We started by first implementing the RTLS in the fibre-optics lab at the Electrical Engineering Department. The implementation mainly includes installing and mounting

the sensors, measuring the sensor positions using laser-based surveying instrument, installing the location engine software, configuring the tags, and finally calibrating the orientation and cable offsets. After the installation, the small-scale effect, large-scale effects and the tracking ability are all studied in the mentioned environment. Finally, obstructed and NLOS scenario were performed to study the performance of the RTLS.

The second part of the thesis contributes to the research by implementing an Approximate Maximum Likelihood Algorithm for Time Difference of Arrival Localization (AML-TDOA). The implemented algorithm extends the work of Chan [Cha 06] to the IEEE802.15.4a UWB channel model. In addition, NLOS mitigation that uses the residual weighting technique [Chen99] is implemented and examined over the UWB channel. Finally, an improved residual weighting algorithm is suggested and implemented.

As shown below, Figure 1-2 summarizes the details of the thesis work.

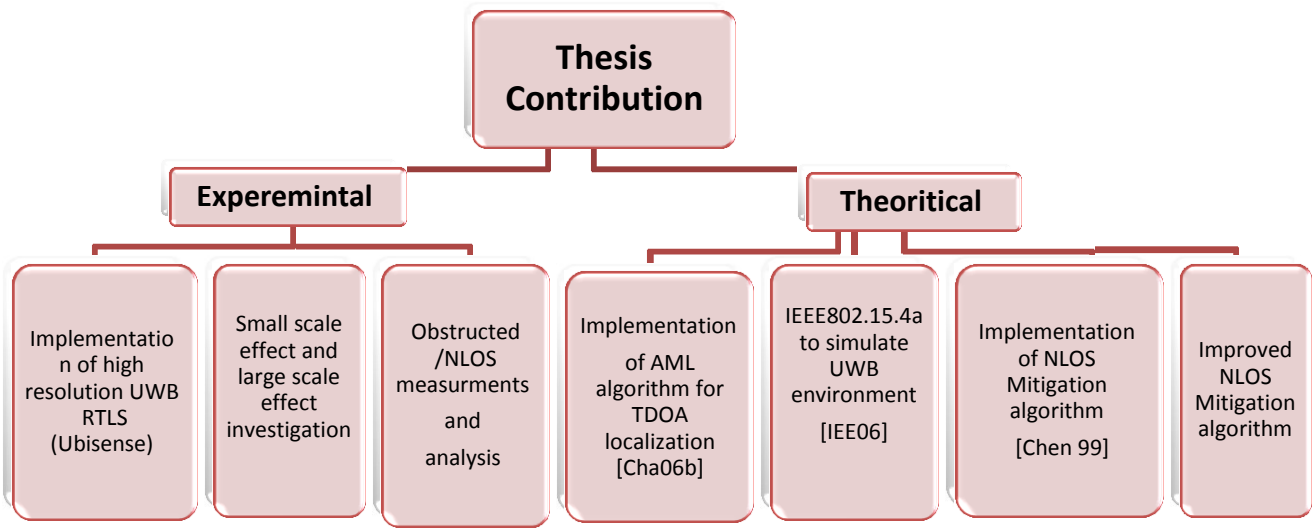

Figure 1-2: A summary of the thesis contribution

1.4 Thesis Organization

After having an introduction, that includes a review of literature and an insight on the contribution of this thesis work, Chapter 2 gives a technical background on ultra wideband localization. This includes an overview of ultra wideband technology and its potential for localization and different location estimation technologies. Chapter 3 discusses the details of the evaluation of a UWB high-resolution RTLS. This will include the system installation, data acquisition and analysis of small-scale, large scale, and obstructed propagation effects .In chapter 4, the implementation of AML-TDOA and NLOS mitigation algorithms are discussed in details with their results. Chapter 5 concludes the work with a summary and gives suggestions for future research.

CHAPTER 2 ULTRA WIDEBAND LOCALIZATION

2.1 Introduction and Motivation

Ultra wideband (UWB) signals are characterized with their very large bandwidth compared to the traditional narrow band signals. According to the U.S. Federal Communication Commission (FCC), a UWB signal is defined as any signal that has an absolute bandwidth of at least 0.5 GHz or a relative (fractional) bandwidth that is larger than 20% [Fcc02]. The absolute (-10 dB bandwidth) bandwidth, B, is known as the difference between the upper frequency f_H of the -10 dB emission point and the lower frequency f_L of the -10 dB emission point; i.e.,

$$B = f_H - f_L \tag{2.1}$$

The relative (fractional) bandwidth, B_{frac} on the other hand, is defined as

$$B_{frac} = \frac{B}{f_c} \tag{2.2}$$

where f_c is the center frequency given by

$$f_c = \frac{f_H + f_L}{2} \tag{2.3}$$

From (2.1) and (2.2) the fractional bandwidth can be expressed as

$$B_{frac} = \frac{2(f_H - f_L)}{f_H + f_L} \tag{2.4}$$

UWB signals occupy a very large bandwidth that results in interference with other existing systems. Therefore, a set of rules are imposed on communication systems transmitting UWB signals. According to the FCC regulations, the average power spectral density (PSD) should not exceed -41.3 dBm/MHz for the frequency band between 3.1 and 10.6 GHz, and should even be lower outside this band, depending on the application [Fcc02].

In time domain, UWB signals are characterized by very short duration waveforms, usually about nanoseconds. Commonly, UWB systems transmit very short duration pulses with a low duty cycle. Such a signaling scheme is known as impulse radio ultra wideband (IR-UWB). For localization application, the focus is to estimate location related parameters of this IR-UWB signal. Those parameters include time of arrival (TOA), time difference of arrival (TDOA), angle of arrival (AOA) or received signal strength (RSS) as will be discussed later in this chapter.

The large bandwidths of UWB signals bring many advantages and application that include [Sah08]:

- ✓ **Penetration through obstacles**: the spectrum includes low frequencies.
- ✓ **Accurate location estimation**: due to high time resolution and multipath immunity.
- ✓ **High-speed data transmission**: can be appreciated from Shannon capacity formula.

- ✓ **Low cost and low power transceiver design:** UWB signals can be transmitted without a sine-wave carrier (carrier-free) and the system is readily in baseband.

For localization systems, UWB provide an accurate, low cost and low power solution. Short-range wireless sensor networks (WSNs) is an emerging application of UWB signals [Gez05]. Some of the applications of UWB WSNs include inventory control, medicine, security, military, search and rescue.

The application offered by UWB WSNs resulted in the formation of the IEEE 802.15 low rate group (TG4a) in 2004 to design an alternate PHY specification for the already existing IEEE 802.15.4 standard for wireless personal area networks (WPANs). The main objective of the TG4a was to provide communications and high precision localization with low power and low cost devices. In March 2007, **IEEE 802.15.4a** was approved as a new amendment to the IEEE 802.15.4. The 15.4a amendment specifies two optional signaling formats based on UWB and chirp spread spectrum (CSS) [IEE06]. The UWB option can use 250-750 MHz, 3.244-4.742 GHz or 5.944-10.234 GHz bands.

2.2 Localization Estimation Techniques

Location estimation of a node in a wireless networks involves a signal exchange between the node, target node to be localized, and a group of reference nodes [Gez08]. The target node can estimate the location of the target node itself, this is called *self-localization*, or a central unit that gathers information from the reference nodes can estimate it and this is called *remote-localization* [Gus05]. In addition, depending on whether the localization is determined directly from the signal traveling between the nodes or not, two different location estimation techniques can be considered as shown in

.Direct localization in which the location estimation is calculated utilizing the full details of the signal travelling between the nodes. Two-step localization, on the other hand, that first extracts certain information from the received signal (e.g. AOA, TOA or TDOA) and

then estimate the location based on those parameters. Although the two-step approach is suboptimal, it has a low complexity than the direct approach. In addition, the performance of the two approaches is very close for signals with high bandwidth (like the case of UWB) and high signal to noise ratio (SNR) [Wei04], [Qi06]. Therefore, the two-step technique is a common one and will be the focus of this research.

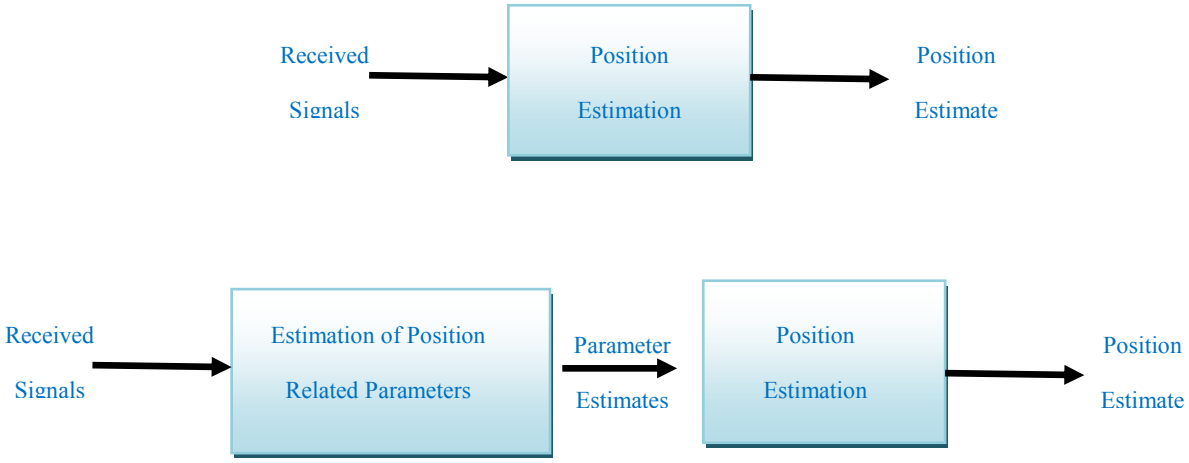

Figure 2-1: (a) Direct localization. (b) Two-step localization

As shown in

-(b), the first step in the two-step localization is calculating the parameters from the signal received from the target node. Those parameters are usually related to the energy, direction or the timing of the received signal. Commonly a single parameter of the received signal is estimated. However, there exist hybrid techniques that estimate more than a single parameter in order to enhance the accuracy of target node location. Brief descriptions of the different parameters are given below:

- ✓ **Received Signal Strength (RSS)**: The energy of the signal changes with the distance and this could help in finding a relation between the received signal

strength and the distance to the target node. In the presence of such a relation, the distance between the nodes can be estimated from the RSS measurement at one of the nodes assuming the transmitted signal energy is known. Commonly, the RSS technique does not provide a high accuracy in the localization due to its heavy dependence on the channel parameters.

- ✓ **Angle of Arrival (AOA)**: The angle of arrival of the received signal to a node can be calculated by deploying an antenna array. The idea is that the difference in arrival times of the received signal at different antenna element contains the angle of arrival information for known array geometry. This technique can provide high localization accuracy especially at high SNR and high bandwidth. However, it adds some complexity and cost due to the deployment of antenna arrays.

- ✓ **Time of Arrival (TOA)**: The time of arrival of a signal travelling from the target node to another reference node can be utilized to calculate the distance between those two nodes. The condition is that both nodes have to be synchronized to avoid an unambiguous TOA estimate. This can be approached by having a common clock or exchanging the timing information. From multipath prospective, TOA is the time of arrival of the first path (assuming LOS between the two nodes).

- ✓ **Time Difference of Arrival (TDOA)**: Another parameter is the difference between the arrival time of two signals travelling between the target node and two reference nodes. The TDOA parameter can only be estimated if there is

synchronization between the reference nodes. One way to estimate TDOA is to calculate TOAs between the target node and the two reference nodes and then obtain the difference that represents TDOA. In addition, TDOA can be calculated by cross correlating the received signals at both reference nodes and obtain the delay that correspond to the largest cross correlation value.

A summary of the different parameters with their strengths weaknesses and usage is given in Table 2-1below.

Estimated Parameter	Characteristics	Strengths and/or weaknesses	Usage
TOA	Uses time information between the reference nodes and the target nodes	It requires perfect synchronization between the reference nodes and the target node	Common in cellular network
TDOA	Difference between TOAs in several reference nodes are utilized	Synchronization is only required between the reference nodes	More common in wireless sensor networks
RSS	The location is estimated based on the attenuation of the signal while propagating form the target node to the reference node	Accurate model is required for reliable location estimation. The mobility of the target node may lead to large errors	Suitable for application that does not require accurate localization
AOA	Uses the angle information to from lines between the target node and the reference nodes and their intersection is used to estimate the location	Antenna array need to be deployed in the reference nodes and that will add to the cost and the size of those nodes	The antenna array deployed in the reference nodes only. Otherwise, the target node size will be large.

Table 2-1: Comparison of different received signal parameters

Depending on the availability of the database (training data), two types of the location estimation schemes can be considered [Gez08]: mapping (fingerprinting) technique and

geometric and statistical techniques. In the following subsections, we explain these techniques.

2.2.1 Mapping (Fingerprinting) Technique

Mapping (or fingerprinting) technique uses a database that consists of previously extracted signal parameters at known reference locations to estimate the location of the target node. A database is obtained during the training (off-line) phase before the real time localization starts. The main advantage of this method is that it provides a very accurate localization even in difficult environment with dense multipath or NLOS propagation. However, the main disadvantage of this method is that it requires a frequent update to the database so that the channel characteristics in the training and localization do not differ significantly and degrade the accuracy.

2.2.2 Geometric and Statistical Techniques

In case of no training data, we can use geometric or statistical techniques as explained below.

2.2.2. (a) Geometric Techniques

In the geometric techniques, the signal parameters estimated from the first step is used directly to calculate the location of the target node. These techniques solve for the location of the target node as the intersection of the location lines obtained from a set of location related parameters at a number of reference nodes. For example, a TOA parameter defines a circle for the location of the target node; hence, three parameter estimates can be used to locate the target by trilateration, as depicted in Figure 2-2 . In the

case of TDOA-based localization, each TDOA parameter defines a hyperbola for the location of the target node. For three-reference nodes, two range differences will define two hyperbolas and their intersection will determine the location of the target node, as shown in Figure 2-3.

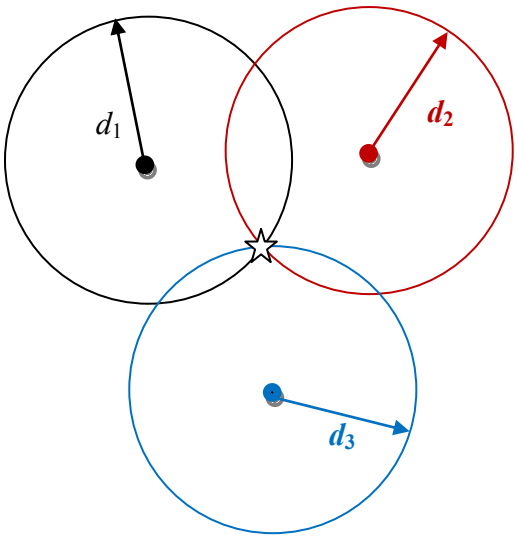

Figure 2-2: Determining the location of the target from TOA measurement and trilateration

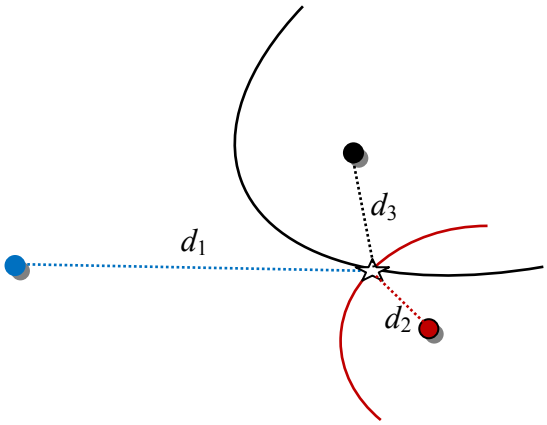

Figure 2-3: Determining the location of the target from TDOA measurement and trilateration

One of the disadvantages of geometric techniques is that they do not provide a theoretical framework in the presence of an error in location related parameters. This occurs when

the lines intersect in an area rather than a point because of an error in estimating the parameters, TDOA as an example. In this case, the geometric method will fail to locate the target node.

2.2.2. (b) Statistical Techniques

These techniques present a theoretical framework for location estimation in the presence of multiple location related parameters with or without errors. The framework can be formulated by considering the following model for the parameters estimated in the first step of a two-step localization algorithm [Gez08]:

$$z_i = f_i(x, y) + \eta_i, i = 1, 2, ..., N_m \quad (2.5)$$

where N_m is the number of parameter estimates, η_i is the noise at the i^{th} estimation, and $f_i(x, y)$ is the true value of the i^{th} signal parameter which is a function of the location target.

Considering the case of TDOA, N_m is one less than the number of reference nodes because TDOA parameter is estimated with respect to a reference node. For the case of TDOA localization $f_i(x, y)$, can be expressed as:

$$f_i(x, y) = \sqrt{(x - x_i)^2 + (y - y_i)^2} - \sqrt{(x - x_o)^2 + (y - y_o)^2} \quad (2.6)$$

where (x_i, y_i) is the position of the i^{th} reference node and (x_o, y_o) is the reference node relative to which the TDOA parameters are estimated.

The statistical approach estimate the most likely location of the target node based on the reliability of each parameter (*i.e.* TDOA) which is determined by the characteristic of the noise corrupting that estimate. Depending on the availability of information about the noise, η, the statistical techniques can be classified as parametric and nonparametric techniques [Sah08]. In the parametric case, the information about the noise distribution is known. However, in the nonparametric case, there is only generic information about some of the parameter of the noise distribution, such as its variance, and they are used to design estimation techniques, such as least squares techniques [Cas06], residual weighting techniques [Che99] and the variance weighted least squares techniques in [Caf98]. In this research, the focus will be on nonparametric way to mitigate the NLOS as will be explained in details in the simulation part.

Figure 2-4 summarizes the different categories of localization techniques and the choice for our research is shown in bold.

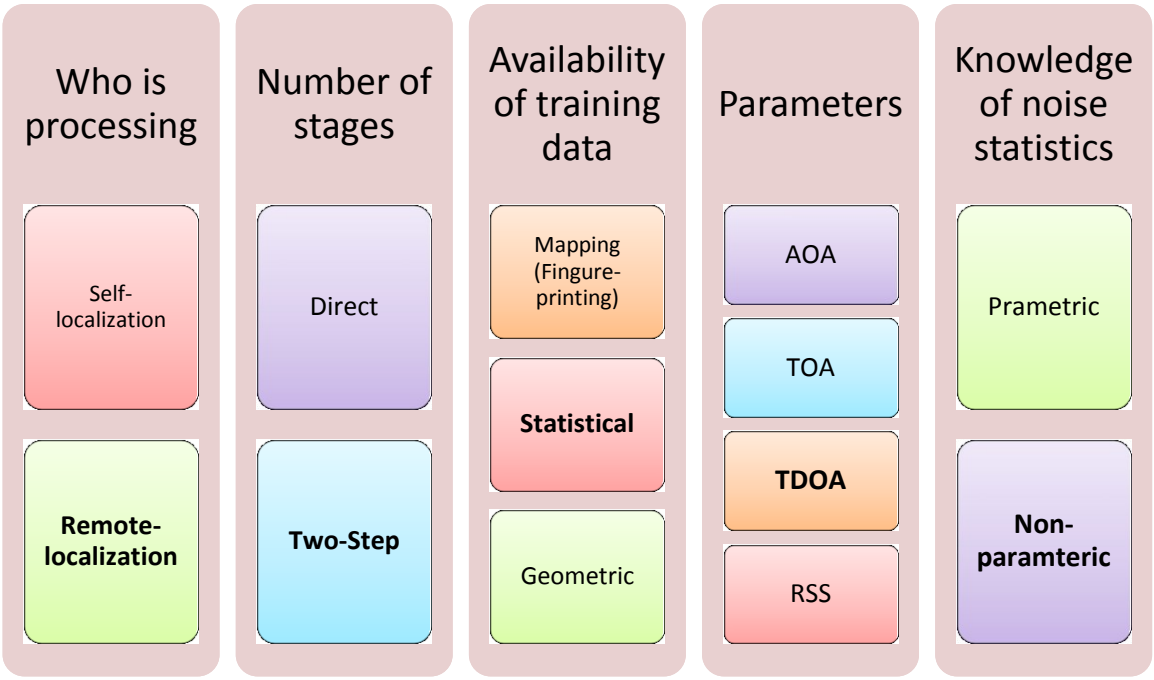

Figure 2-4: Summary of different categories of localization techniques

2.3 Sources of Errors in Time Based Ranging

An accurate TOA estimation and hence an accurate TDOA estimation can be performed with the assumption of having a single-path propagation environment with no interfering signals and no obstacles between the nodes. However, in the practical situation, signals arrive through multiple paths and there are always obstructions or obstacles in the environment. This problem appears in wireless communication technologies like UWB. In the following subsections, we discuss the main sources of errors in wireless localization, namely: multipath propagation, multiple access interference, obstructed and NLOS propagation.

2.3.1 Multipath Propagation

In a multipath environment, the transmitted signal will reach at the receiver through different paths as depicted in Figure 2-5 below. Due to the high resolution of the UWB signals, the different paths are usually resolvable at the receiver. However, in narrowband systems, the paths will overlap causing an error in estimating the TOA. In the UWB case, first path detection algorithms can be used to get an accurate estimation of the TOA and hence an accurate estimation of the TDOA [Lee02], [Guv05], [Gez05], [Yan05].

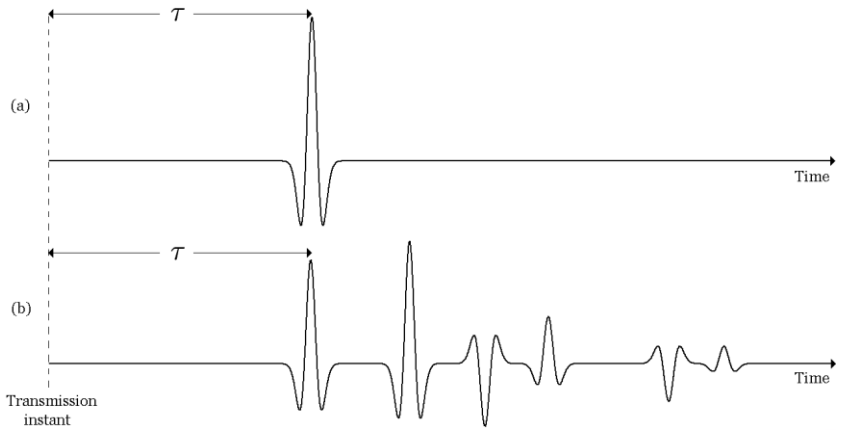

Figure 2-5: a) Received signal in single path case. b) Received signal in multipath case [Gez09]

2.3.2 Multiple Access Interference

Multiple Access Interference (MAI) is mainly due to the existence of many users in the same environment and that might affect the accuracy of estimating timing parameters whether TOA or TDOA. Various mitigation techniques exist in the literature to reduce this effect. Among those techniques are non-linear filtering and training sequence design which are commonly applied [Sah06], [Yan05].

2.3.3 Obstructed and NLOS Propagation

The presence of obstacles between the target node and the reference node will obstruct the line-of-sight (LOS) between them. As a result, the direct signal component is attenuated significantly such that it becomes weaker than some other multipath components or the receiver cannot even detect it. For the first case, first-path detection algorithms can still be utilized to estimate the TOA or the TDOA for accurate localization. However, if the receiver can detect an indirect path rather than the direct path, the delay will not represent the true TOA and it includes a positive bias called non-line of-sight (NLOS). Mitigating NLOS errors is one of the most challenging tasks in accurate TOA estimation for accurate localization.

2.4 Practical Considerations

In this section, the practical issues related to the design of UWB ranging signals are considered.

Although high time resolution of UWB results in very precise TOA estimation and hence an accurate target localization, it puts certain practical challenges. First, clock jitter becomes a significant factor that affects the accuracy of localization systems [Shi03]. UWB pulses have short durations and clock inaccuracies can affect the TOA estimation and hence the localization of the target. In addition, high time resolution of UWB signals makes it impractical to sample above the Nyquist rate. TOA estimation schemes should make use of low rate samples.

In order to meet some performance requirements, UWB signals need to be designed properly. One of the parameters that play an important role is the time duration of the UWB signals [Sah08]. As the duration of the signal increases, the accuracy of estimating TOA increases accordingly and this will lead to accurate target localization. Considering the general UWB signal structure depicted in Figure 2-6 below, where T is the duration of the signal, the idea can be explained using the following equation (2.7) shown below.

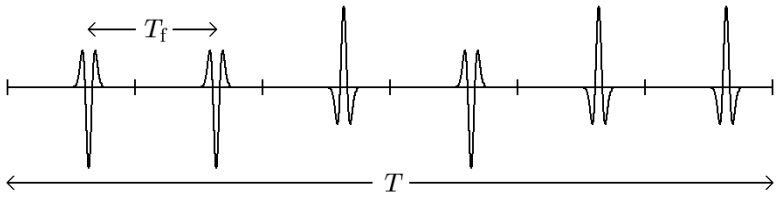

Figure 2-6: An example of UWB signal [Gez09]

The equation relates the accuracy of the TOA estimation to both the SNR and the effective bandwidth, B of the UWB signal. Therefore, one can understand from the equation that the increase in the SNR will result in a better TOA estimation and the same analogy is true for the effective bandwidth. As known from the theory, the energy of the signal is related to the power and the time duration of the signal. Therefore, an increase in the time duration would result in increase in the energy of the signal and hence an increase in the SNR. The final resultant is an increase in the accuracy of estimation and localization.

$$\sqrt{Var(\hat{\tau})} \geq \frac{1}{2\sqrt{2}\pi\sqrt{SNR}\ B} \tag{2.7}$$

The UWB system sends a pulse per frame. A series of pulses are sent to represent a single symbol. Referring to Figure 2-6 again, we can show that the relation between the duration of the signal and the frame width as, $T = N_f T_f$ where N_f is the number of frames T_f and is the duration of each frame. Designing the UWB signal requires a proper selection of the frame duration to avoid reaching above the allowed upper limit by the FCC of UWB signals. It is known that the energy in a pulse is proportional to its duration. Therefore, an increase in the frame duration might lead to a power reaching above the upper limit allowed by FCC.

After the determination of the time duration of the signal T and the frame duration T_f , it is also important to choose the proper pulse code for the UWB signal that is implemented by the sequence a_j in the in equation (2.8).

$$s(t) = \sum_{-\infty}^{+\infty} a_j \omega(t - jT_f) \qquad (2.8)$$

Pulse coding is important for location estimation as it provides robustness against multipath and MAI [Sah08].

CHAPTER 3 IMPLEMENTATION OF UWB REAL TIME LOCATION SYSTEM

3.1 Introduction

Ultra wideband technology provide a real-time location system (RTLS) which delivers very high positional accuracy in traditionally challenging environments at reliability levels unachievable by legacy technologies such as conventional RFID or WiFi. When embedded in production processes, the UWB system provides location aware support to workers, reducing defects caused by human error and cutting down the time needed to execute a particular task. The acquired system is based on Ubisense®. This system delivers a 15cm 3D positional accuracy in real-time which is enabling a number of new applications including: precision device location in space and time, providing the location of a pallet of goods placed on a warehouse shelf, automatic context sensitive proximity detection between objects, identification and location of cars in finishing bays, and determining if employees have all reached designated areas [Alo09].

The system in its 7000 Series is composed of three main components: active tags (battery powered) which transmit UWB pulses used to determine their location; sensors mounted on fixed infrastructure that receive and evaluate the signals from the tags; a software platform to aggregate the positional data generated, presenting, analyzing and communicating information to users and relevant information systems. The tags transmit UWB pulses of extremely short duration which are received by sensors and used to determine where the tag is located using a combination of measurement methods. The use

of UWB together with the unique sensor functionality ensures both the high accuracy and the reliability of operation in challenging indoor environments where there are often disturbing reflections from walls or metal objects. Tag locations are sent via standard Ethernet cable or wireless LAN to the Location Engine software that aggregates the data and passes the information to an external program or to the Location Platform for visualization and spatial processing. The visualization module displays the tags in real-time as they move around the reference grid, irrespective of which cell currently contains them.

Ubisense provide a research package to allow researchers to develop their positioning algorithms and examine the details of the positioning process.

The objective of this part of the project is to install and investigate the accuracy of a high-resolution UBISENSE real time location system that works based on UWB technology. This part involves understanding how the system works and how to install it. It also includes finding the probability of error under different scenarios like non-obstructed, obstructed, and NLOS scenarios. Moreover, the work includes the impact of different conditions and filters on the performance of the system tracking ability.

The UBISENSE real time location system can be divided into two main parts. These parts are the sensor network hardware part, and the location engine software platform. In this section, we are going to introduce these two parts and their sub-parts.

3.2 The RTLS: Hardware Part:

The sensor network part is the hardware part of the system that gathers the readings and it consists of tags, sensors, location engine cell, timing cables, sensor power and networking.

3.2.1 Tags:

Tags are the portable devices that transmit UWB signals that will be detected by sensors. They are the moving parts that their positions will be estimated by the system. They come in two forms, which are slim and compact tags see Figure 3-1 .While the features present on each type differ but the function of both types is the same. The tag operates using two separate radio channels: a bidirectional conventional telemetry channel and a transmit-only UWB channel. Since there is only a single UWB channel, only one tag can be located at a time in each location engine cell.

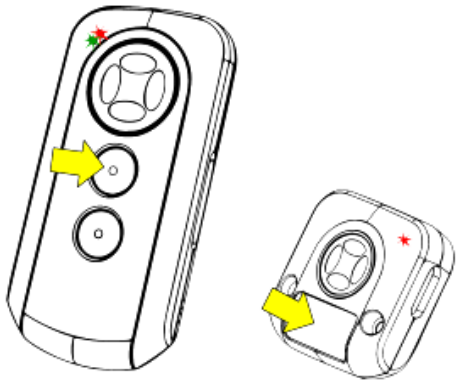

Figure 3-1: The slim tag and the compact tag [Ubi11]

3.2.2 Sensors

Sensors are the hardware parts of the system that receives the signals transmitted from the tag. They should be provided with power, networking cables and timing cable connections. Sensors are organized in cooperating sets called location engine cells, each one of them has a single master sensor and a number of slave sensors. In our project, we used four sensors; three are assigned as slave sensors while the fourth one is the master sensor. The master sensor is needed to calculate the TDOA.

3.2.3 LocationEngine Cell

A location engine cell consists of one or more sensors connected together into a single operating unit. Slave sensors in a cell share information with the master sensor of the cell, where it computes tag locations. Each tag registers with its location engine cell and is inserted into the schedule for that cell. The schedule determines when the tag should emit UWB to be located by the cell. The schedule is already optimized to give each tag as close as possible to its requested service. When a tag emits UWB signal, the signal is going to be picked up by one or more of the sensors in the cell. The slave sensors decode the UWB signal and send the angle of arrival and timing information back to the master sensor by Ethernet. The master sensor accumulates all sensed data, and computes the location of the tag, and delivers the location to the configured sink location. In a full UBISENSE platform, the sink address is automatically set for each location engine cell.

3.2.4 Master and Slave Sensor

Physically the master sensor is the same as a slave sensor. It is only configured to be a master sensor when setting up the cell plan. One of the sensors is set up to be the timing source and generate the timing signal for the synchronization of the rest of the sensors in the cell.

3.2.5 Timing Cables

Timing cables run between each of the slave sensors in a cell and the cell master sensor to provide synchronization between them, which is an important factor in calculation TDOA. A timing cable can be safely run up to 100 m. Figure 3-2 and Figure 3-3 show the connections of timing cables.

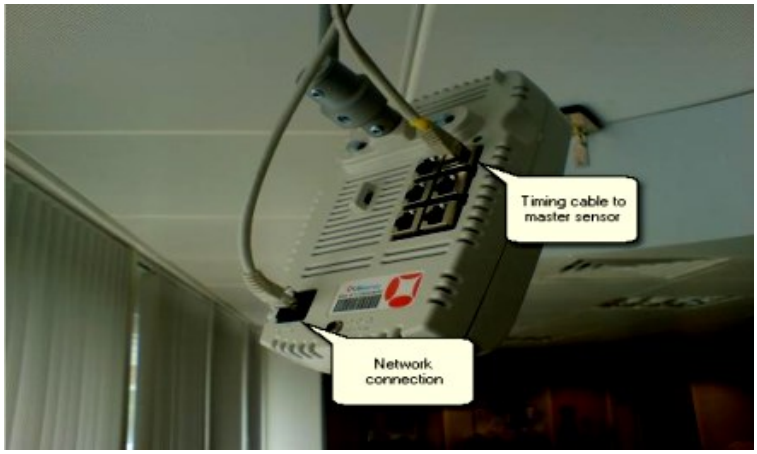

Figure 3-2: Timing cable and network cable on a slave sensor [Ubi11]

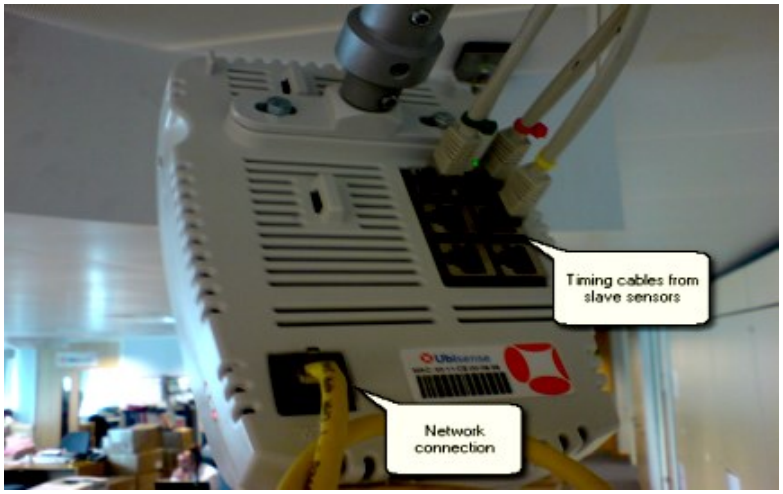

Figure 3-3: Timing cables and network connection on a master sensor [Ubi11]

3.2.6 Sensors Power

Sensors are powered using Power over Ethernet (PoE). This supplies low voltage DC to the devices using spare wires in CAT5 and higher cables. PoE capable switch is directly connected to each sensor. The switch must support 802.3af standard. Each UBISENSE Series 7000 sensor will drain under 7-W power when running. When using a POE switch, the sensor will start to boot as soon as the network cable is attached. Most POE-capable managed switches allow POE to be disabled and enabled per switch port, from network management software or a web interface. This is a convenient way of power-cycling sensors that have been installed at inaccessible locations.

3.2.7 Networking

Sensors are connected by standard 100 BASE-TX Ethernet to the master and the platform server. The sensors can be connected with either a switch or a hub. Sensors support POE, in which case the switch must be a POE capable switch. **Error! Reference source not**

ound. below shows Ethernet connections for a four-sensor location engine cell and the platform server. Note that the sensors require a Dynamic Host Configuration Protocol (DHCP) server to assign their network configuration.

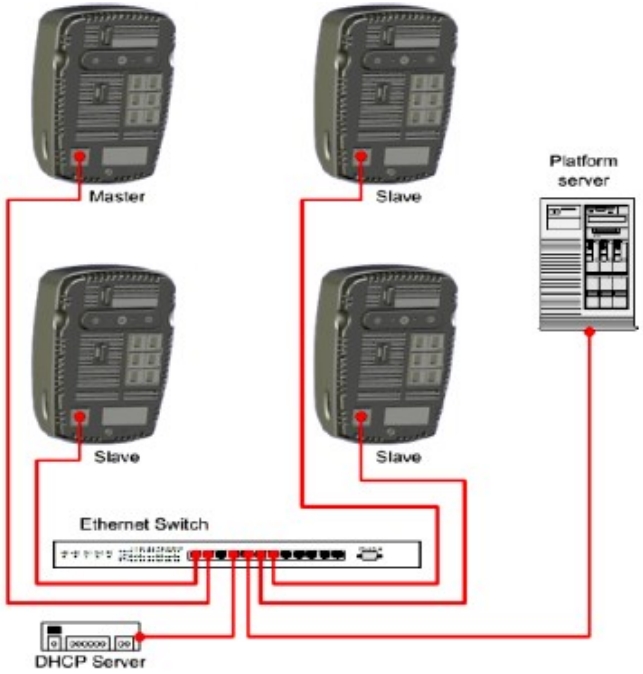

Figure 3-4: Connections for a four-sensor location engine cell and the platform server [Ubi11]

3.3 The RTLS: Location Engine Software Platform

Location Engine Software Platform (LESP) is the software that is provided with the UBISENSE location system to collect real time data from the sensor. The LESP has its own built-in algorithms that will estimate the location of the tag. The following steps are to be conducted before the software is run:

1. All network connected to the computer must be disabled.
2. All antivirus or firewall programs must be disabled.

3. The computer must be connected to the switch that supports PoE.
4. All automatic IP address assignment must be disabled and the following IP address and subnet mask must be put.

IP Address	192.168.0.2
Subnet Mask	255.255.255.0

3.3.1 Platform Control

When the platform control is opened, the core server and the service controller are run. By doing this, the computer will assign each sensor an IP address. The LEDs will start to flash. When they go steadily green, the location engine configuration can be started.

3.3.2 LocationEngine Configuration

This is the core of the tracking system. The cell being monitored can be shown here and other options as listed below:

This is the core of the tracking system. The cell being monitored can be shown here and other options as listed below:

1- **Importing Sensors**: Sensors can be added manually either individually or multiple at one time. This will be done by entering the MAC address of each sensor. The properties of each sensor can be modified any time like xyz coordinates and the tilt of status tab that will give summary of sensors properties like its MAC, in which cell, last time seen and its IP address.

2- **Adding tags**: Tags can be added individually or as group. The update rate can be adjusted for the case of fast or slow tag motion and the speed threshold must be specified so any speed below this will be considered as slow and slow update rate will be used whereas any speed greater that the threshold will be considered as fast and fast update rate will be used. Each tag can have a different filter- used for fine-tuning- which will apply some parameters values on it to give better accuracy. Other properties of the tags can be shown from the tag tab, like battery information of each tag and its status.

3- **Owners tab**: Is used to indicate the one who is carrying the tag.

4- **Cell calibration**: In full calibration, a tag is carried around the cell at fixed height in different points where the tag is clearly seen by the sensors as much as possible. If the full calibration fails to find good solution for cable offsets then dual calibration will be done.

5- **Dual calibration**: This is done when full calibration fails, it computes the cable offsets between two pairs of sensors (usually master & slave). If it is not possible to calibrate a sensor with the master it can be calibrated with a slave sensor which is already calibrated with the master. A calibration point with known coordinates must be known in order to perform this type of calibration.

6- **Tag monitoring**: When a tag is to be monitored, its serial number is chosen. In the cell map, it will be shown as a red dot and its coordinates will be shown in the main window. It is also possible to track all tags by leaving the tag box empty (no serial number ID entered). The events taken during tracking can be saved in an Excel sheet

from the event menu for further analysis. In the cell map, we can enable or number ID entered). The events taken during tracking can be saves as excel sheet from the event menu for further analysis. In the cell map, someone can enable or disable the tag symbol, AOA (green line), TDOA (blue curve) , peak to peak offset (PPO), UWB code which will be shown as numbers at each sensor and leave trail which will show tags track.

7- **Log tab**: Shows different messages from the sensors. It helps to check if some errors or warnings exist.

8- **Controlling the view**: It is possible to zoom in or out the cell map and also to show its 2D or 3D view

3.3.3 Calibrating the RTLS

The calibration for the RTLS involves the calibration for the background noise, the orientation of the sensors, and the cable offset.

When calibrating the sensor noise threshold, all the radio communication between the tags and the sensors are disabled to accurately calibrate the background noise. The noise level heavily depends on the environment.

To calibrate the sensors orientations and the cable offset several stages are involved. Calibrating the sensor requires fixing its three angles, elevation, azimuth and tilt or rotation. Prior to calibration, it is important to choose the origin and the coordinate system in the environment. The origin is defined to be approximately on the center of the lab. Right-hand rule is followed in determining the x, y and z-axes.

To start the calibration process we need firstly to choose three (one for each slave sensor) different locations (called calibration points). Those locations need to be relatively far from each other (2 meter is enough according to Ubisense manual). Each of these calibration points is used to calibrate one of the slave sensors. Therefore, each point should have a line of sight to both the intended sensor and the master sensor. In order to get an accurate calibration, we also used a laser based Total Station surveying instrument to calculate the location of the calibration points.

To calibrate a sensor, the location of its calibration point (x, y and z values) will be entered to the system and the system will calibrate the location, the cable offset and the angles of the sensor. Note that the calibration process may fail several times before getting the right calibration. This is mainly due to the complex environment in the lab.

3.3.4 Challenges faced when configuring the RTLS

It is worth to mention that installing the RTLS was a challenging task.

1. If problem is faced with networking, a full knowledge of Ethernet and (Internet Protocol) IP networking is needed to resolve the issue. In our case, a multitasking was caused networking problems. It was more than a month of experiments and communication with the manufacturer before this issue was resolved.
2. We had to develop our own data acquisition and formatting to process the output of the positioning engine. The results in Section 5 are mainly generated using Matlab.
3. Some Intellectual Property (IP) related issues limited our access to the positioning algorithm.

4. Calibration: in order to maintain the best localization reference we had to seek some help from the Civil Engineering Department and a Total Station system based on laser was used to calibrate the system.

Figure 3-5 shows part of the lab environment. After successfully installing the system, the location of the tag can be determined using the software as shown in Figure 3-6.

Figure 3-5: Pictures of the lab environment

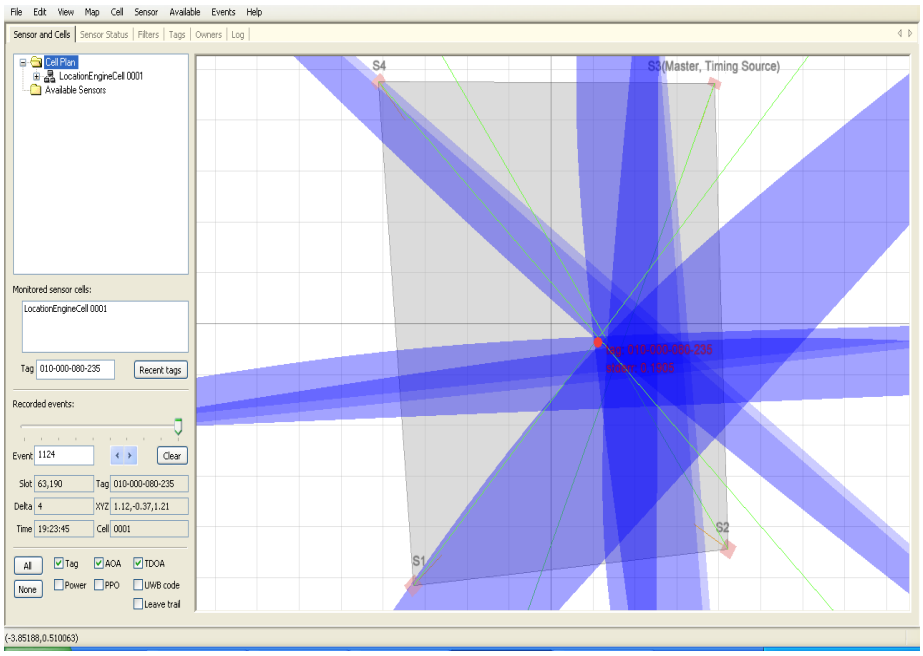

Figure 3-6: Ubisense Software

3.4 Real Time Location System and Experimental Evaluation

Positioning experiments were performed covering the whole laboratory room (Building 59, room 0020, KFUPM) where the system was installed. The room has a length of 10.8m and a width of about 8.7m. There are five metallic tables and a column in the middle of the room. The dimensions are shown in Figure. On the same figure, the sensors are shown and the y-axis is labeled with numbers while the *x*-axis is labeled with letters for ease of referencing. Measurements were conducted to examine large-scale effect, small-scale effect and to study the tracking ability of the system.

Data collection and measurement execution go through different steps. First**,** identifying the cell where the system is installed. This step could be considered as the planning phase and it includes different stages starting by identifying the origin of the cell to be used as

the reference for all test points. The origin should be selected to have a LOS to all sensors. Then, from the origin of the cell, the positive directions of *x*-axis, *y*-axis and *z*-axis are determined following the right hand rule. Finally, the system is calibrated so that it can measure tag locations accurately.

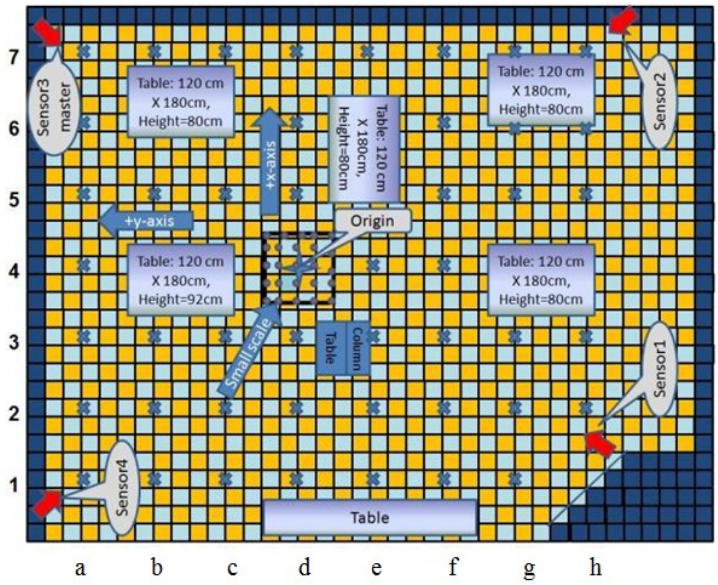

Figure 3-7: Points distribution in the cell (top view)

3.4.1 Large Scale Effects

The objective of the large-scale analysis is to study the impact of large movements on the positioning accuracy. In general, measurements should be averaged out to remove the impact of multipath and other small-scale effects. UWB signals are immune to multipath as will be illustrated when studying the small-scale effects.

Based on the calibrated reference point, a grid was sketched as shown in Figure 3-7. Data was collected for all possible points separated by a distance of 1.2 m in both *x* and *y* directions. This should results in 56 points around the whole cell. However, due to

blocking objects, only 49 points were taken. Missing points were considered as NLOS scenarios.

The error distribution in *x*-component is shown in Figure 3-12 where *x*-axis corresponds to 'numbers 1-7' and 'letters a-h' corresponds to *y*-axis as shown in Figure 3-7. Areas with blue color indicate the least error whereas areas with red color indicate the highest error. Errors are given in cm and the color bar to the right of Figure 3-12 indicates the range of the error and their corresponding color. Most of the points were positioned with error which is less than 15 cm. Five points have errors exceeding 30 cm. Maximum positioning error was found to be 50 cm. This could be due to obstructed or NLOS scenario. The point is at the border of the cell and some reflecting materials like metallic tables exist in the room.

Figure 3.9 shows the error distribution of the large-scale data in *y*-component. Most of the values are less than 15 cm. The error in *y*-component is less than that in *x*-component as it can be noticed by comparing Figure 3.8 and Figure 3.9 where the maximum reached about 30 cm.

Figure 3.10 shows the error distribution in the radial component where the radial component is calculated as $r = \sqrt{x^2 + y^2 + z^2}$. The error in the radial component is composed of *x*, *y*, and *z* component and is greater than any of them. The areas that suffer more error are those at the border of the cell or those close to the metallic tables. This is expected since at the border, the tag is not seen properly by all the sensors while for the metallic tables they will act as reflectors.

Figure 3.11 shows the exact location of the tag marked by the symbol '+' and the estimated location which is marked by the symbol '*'. Most of the estimated locations are reasonably close to the real location. The range of the error is less than 20 cm for most of the points.

In addition, some points for NLOS are shown in the same figure. These points are marked by a symbol of triangle for exact location and a red square for their estimations. A similar result can also be observed in this case except for only one location that is close to the top left that is far from the actual location.

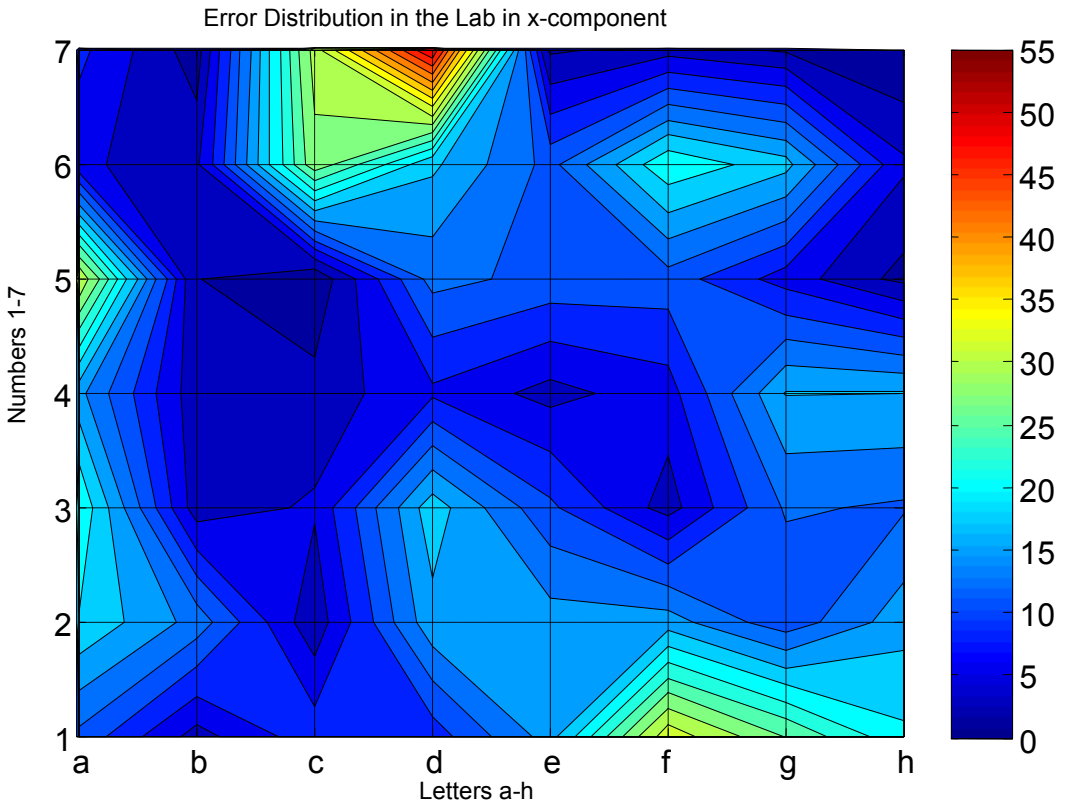

Figure 3.8: Error distribution in *x*-axis

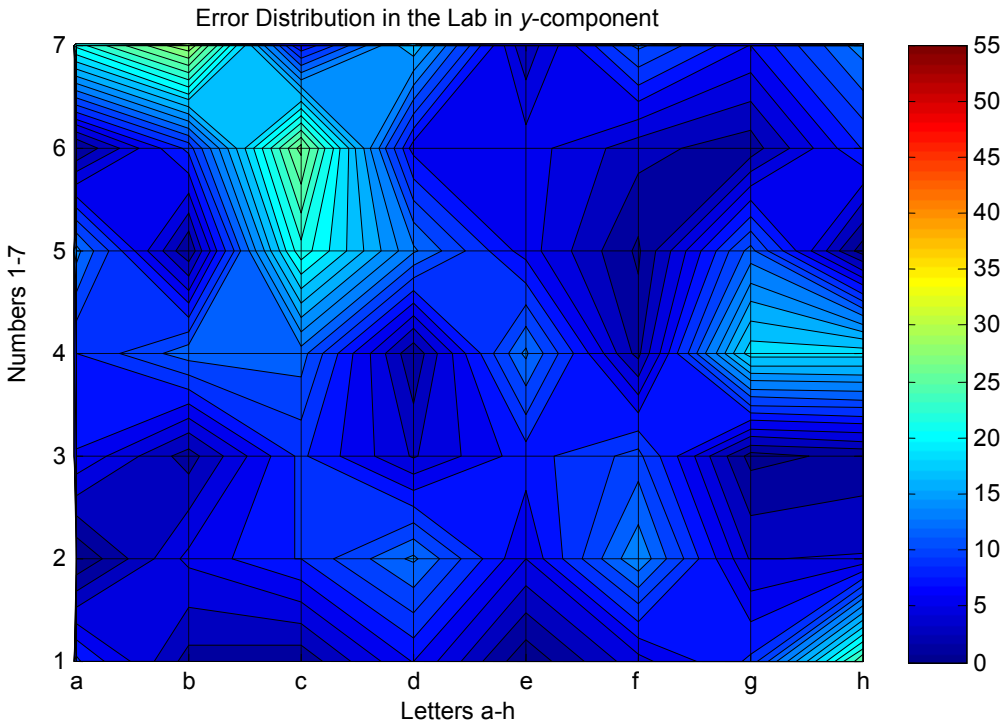

Figure 3.9: Error distribution in *y*-axis

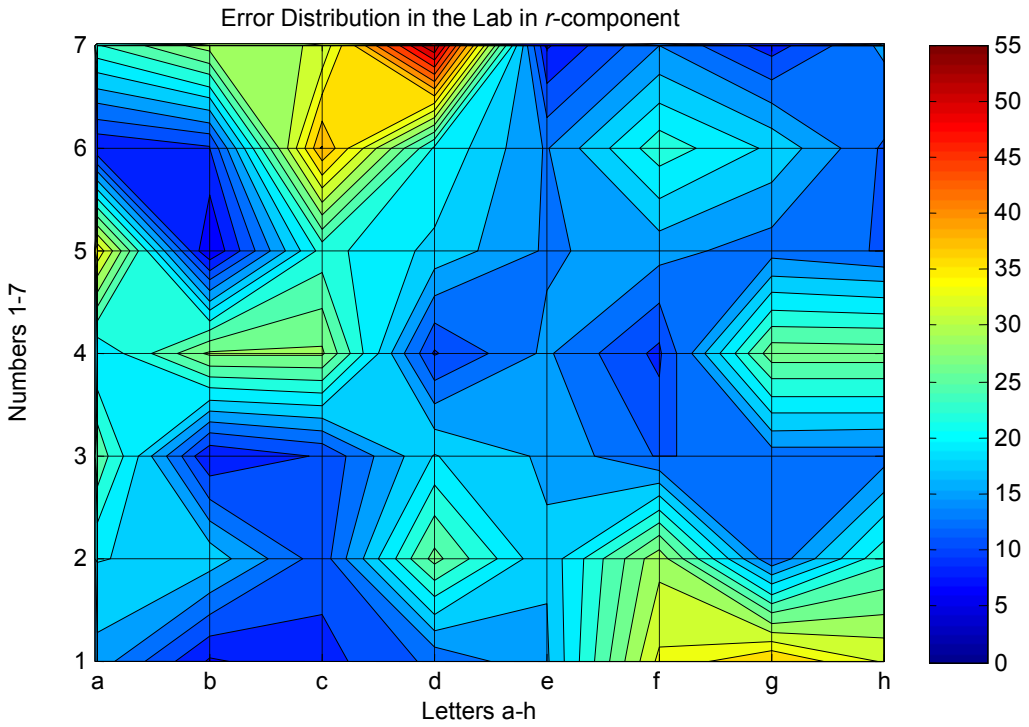

Figure 3.10: Error distribution in *r*-component

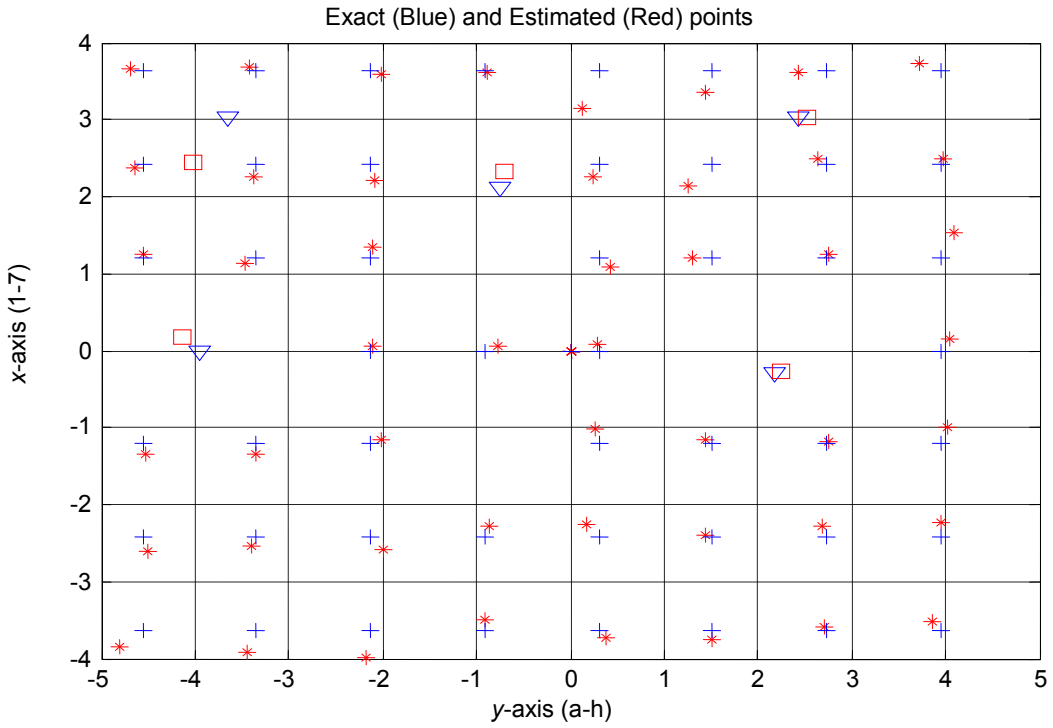

Figure 3.11: Exact and estimated location of the tags

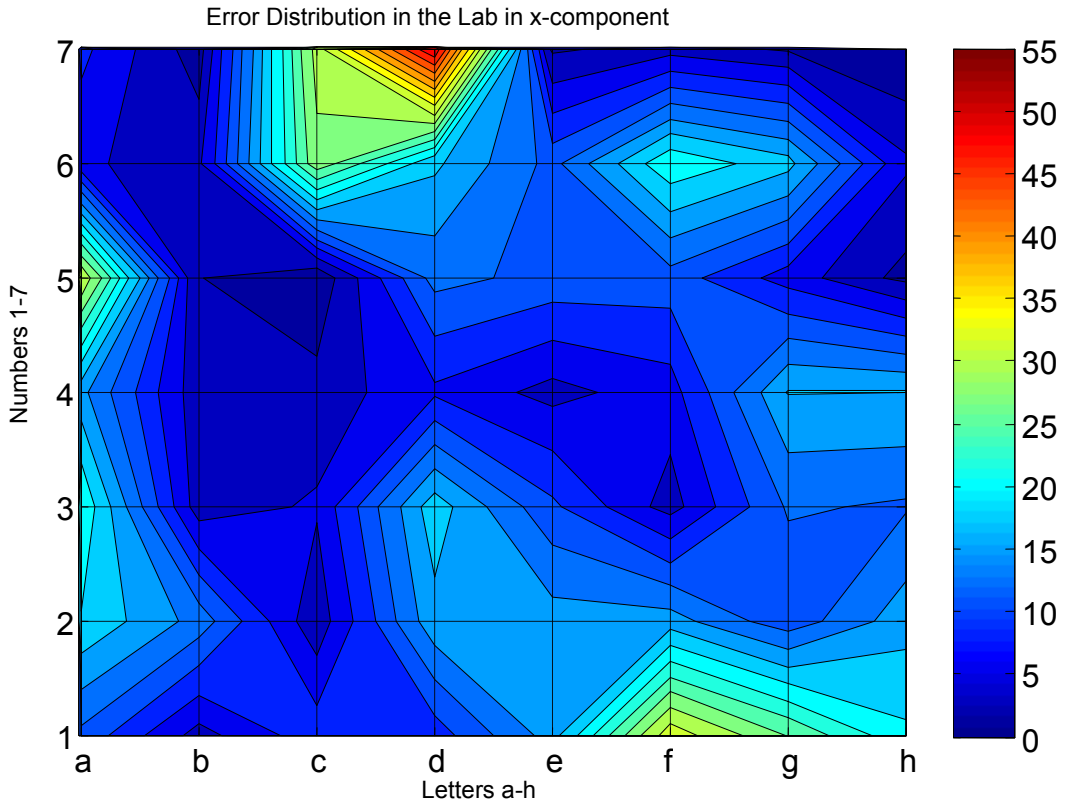

Figure 3-12: Error distribution in *x*-axis

3.4.2 Small Scale Effects and Multipath Immunity

Small-scale effect was tested on an area of about 0.607m^2 near the origin as shown in Figure 3-7. This area was divided into 25 different points separated by a distance of 0.152m in both *x* and *y* direction. To study the small-scale effect the choice of the spacing should be related to the wavelength of the carrier frequency. In case of UWB, the center frequency may be used instead. The height (*z*-direction) was kept fixed for all of them at 1.43m, which is close to the height of mobile phones during calls.

Figure 3.11shows the small-scale points and their estimated locations. Every two points with the same color and shape corresponds to the exact and estimated points. The darker point represents the exact position. Some of the points are estimated with errors less than 10 cm. Few points are estimated with larger error because these points are not seen by sensor-1 due to the concrete pillar in the middle of the room and hence the signal is reflected and results in larger estimation error. Most of the points suffer from a fixed bias, which could possibly reflect a calibration error. We observe that UWB positioning is immune to multipath and small-scale effects. Some points that demonstrated different errors are due to pillars obstruction.

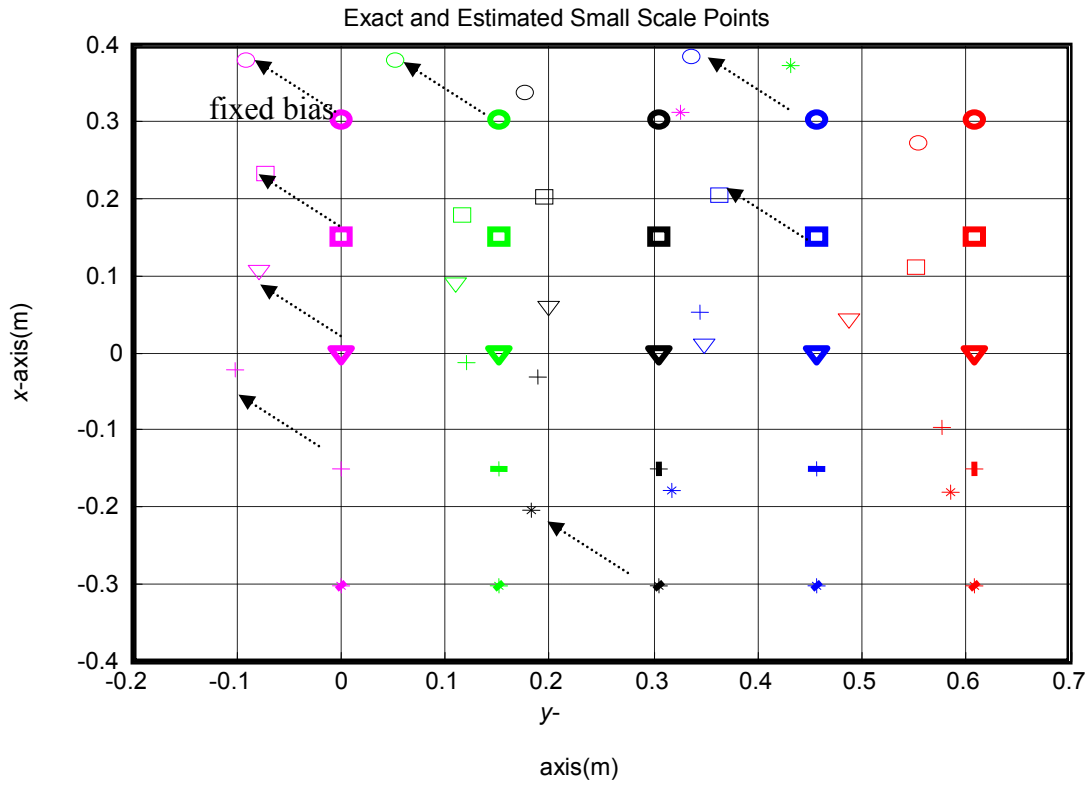

Figure 3.13: Exact and estimated location of the Tag (same shape & color are for one point)

In the large-scale case, the system is tested for large separation distances and in the small-scale measurement; it is tested for small separation distances. In the following sections, the system performance is tested for different NLOS and obstructed scenarios that are the major problems in high resolution positioning.

3.4.3 Obstructed Sensors

The system performance was tested when one sensor is blocked by wooden plate or Aluminum plate (see Figure 3.14). The tag was placed in a location where already a LOS reading with no blocking was taken so that the blocking effects can be investigated. This point was kept fixed when each of the four sensors was blocked and this point was taken as point (0, 0, 1.43) m. Only one sensor is blocked at a time.

Figure 3.14: Obstructed sensor (sensor blocking with a wooden plate)

3.4.3. (a) The Effects of Blocking Sensors with Aluminum

The following set of figures show the effect of blocking one sensor with Aluminum plate. The probability density functions (pdfs) are plotted with and without the sensor blocking.

When sensor 1 was blocked with an Aluminum plate, the range of the error expanded as shown in the Figure 3.15. Blocking the sensor will not make big difference because the sensor is already blocked by the column in the middle of the cell.

When sensor 2 is blocked, the error distribution changes very much. The error increases in *x* and *y* component. This happens because the sensor has a line of sight to the tag. (see Figure 3.16).

Blocking sensor 3 has resulted in larger errors in all the components because it is the timing source (see the two parts of Figure 3.17). So, if the signal arrives late to this sensor then the other estimations will be affected because the TDOA technique is used.

Blocking sensor 4 also change the error range and the mean of the error. This error is due to error in both *x* and *y* components as can be seen from the second plot of Figure 3.18.

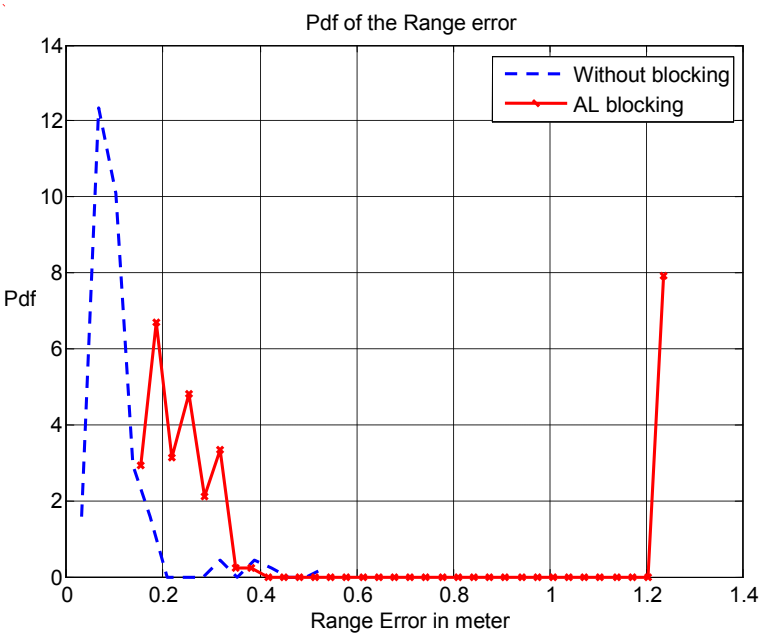

Figure 3.15: The effects of blocking sensor 1 with Aluminum plate

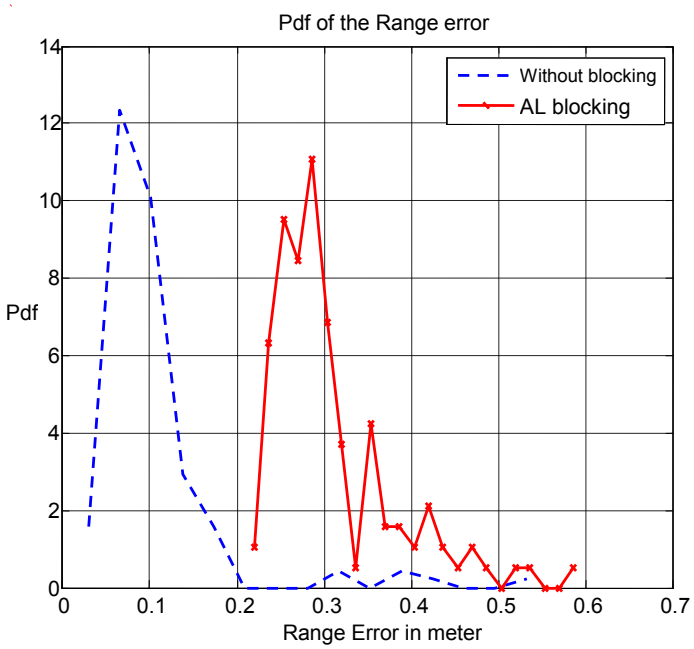

Figure 3.16: The effects of blocking sensor 2 with Aluminum plate

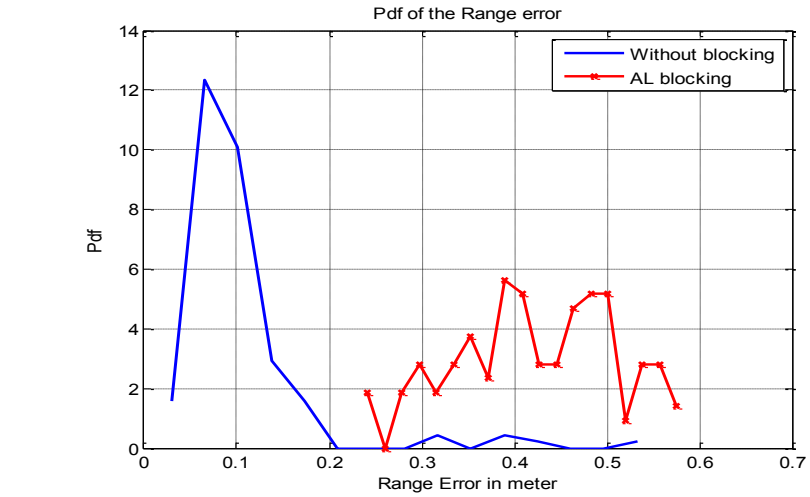

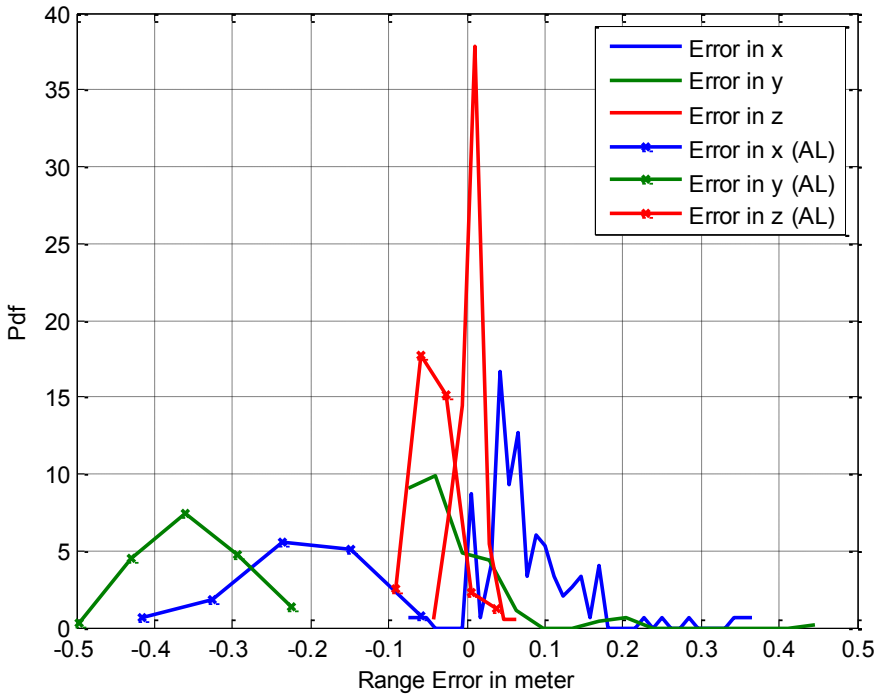

Figure 3.17: The effects of blocking sensor 3 with Aluminum plate

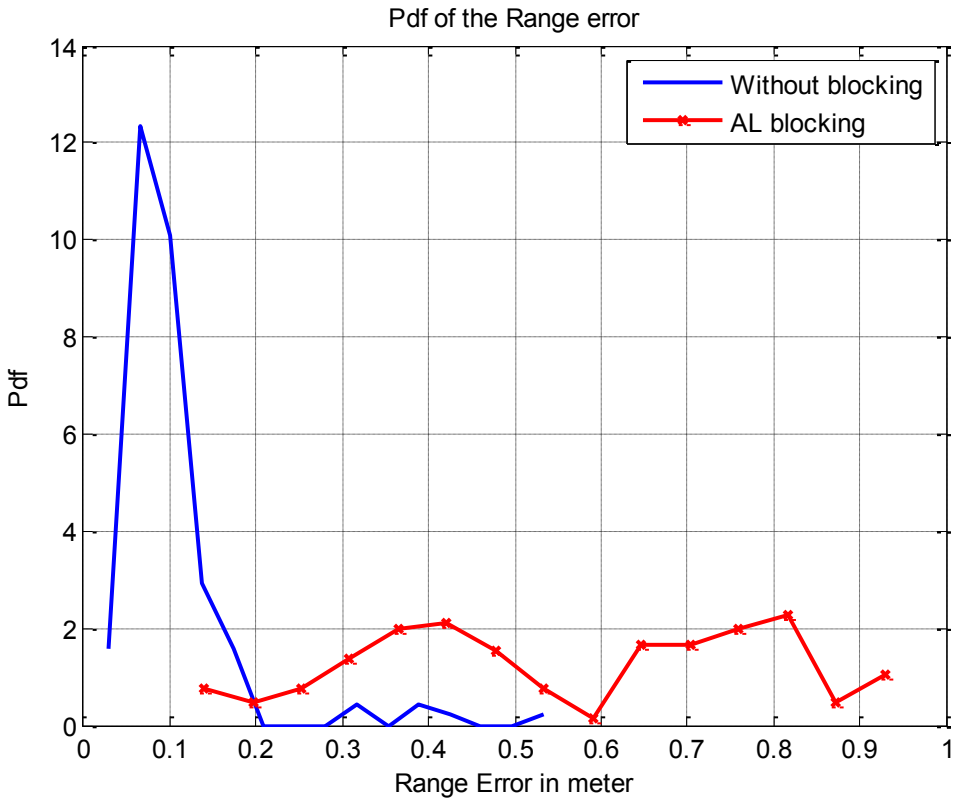

Figure 3.18: The effects of blocking sensor 4 with Aluminum plate

3.4.3. (b) Results of Blocking the Sensors by Wooden Plate

The following sets of figures show the effect of blocking one of the sensors with a wooden plate. Blocking any sensor with the wooden plate has less effect compared with aluminum. The impact of blocking sensor 2 and 3 with wood are shown in Figure 3.19 and Figure 3.20, respectively. This is because the wood introduces less delay and attenuation for the waves.

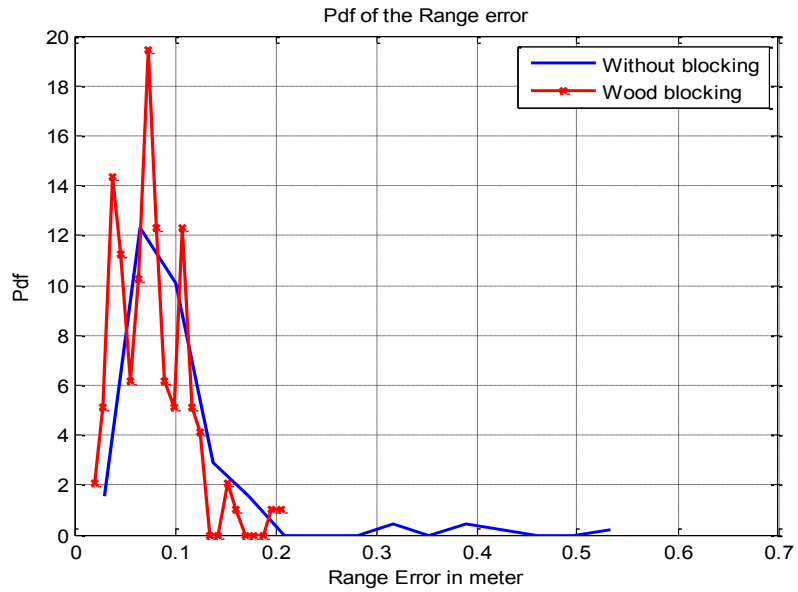

Figure 3.19: The effects of blocking sensor 2 with wood plate

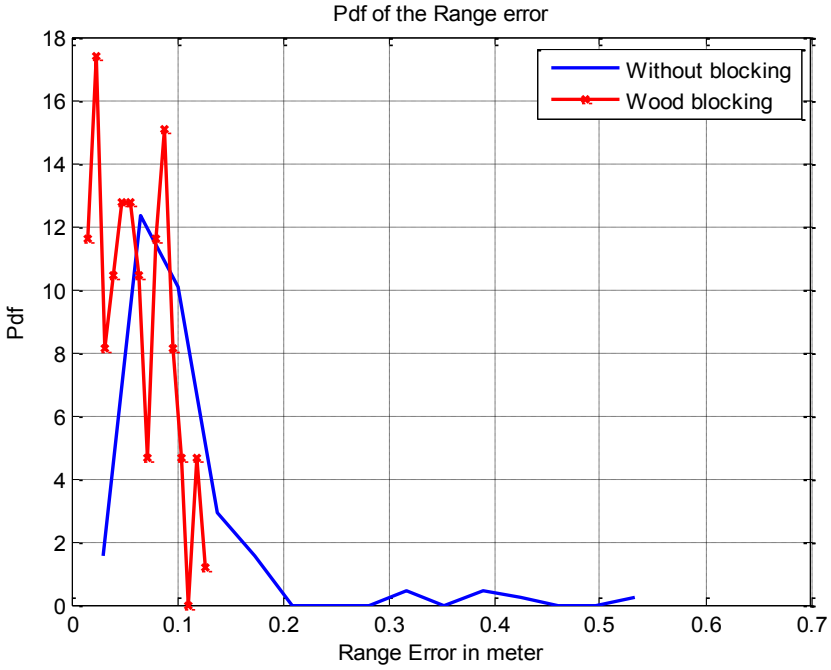

Figure 3.20: The effects of blocking Sensor 3 with Wood plate

3.4.4 NLOS and Covered Tags

The system performance was tested when the tag is covered by different types of materials such as wood box and bowl made of steel or glass (see Figure 3.21 and Figure 3.22). The box made of wood has dimensions of 16cm in length and width and 20cm in depth while its thickness is 2cm.

The bowl made of steel has a top diameter of 16 cm and a depth of 7 cm with thickness of 2 mm. The glass bowl has a top diameter of 12.5 cm and a depth of 5 cm and its thickness is about 3 mm.

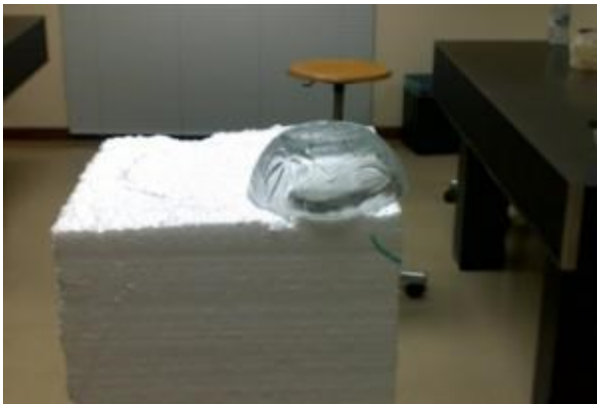

Figure 3.21: The tag is covered by the glass bowl

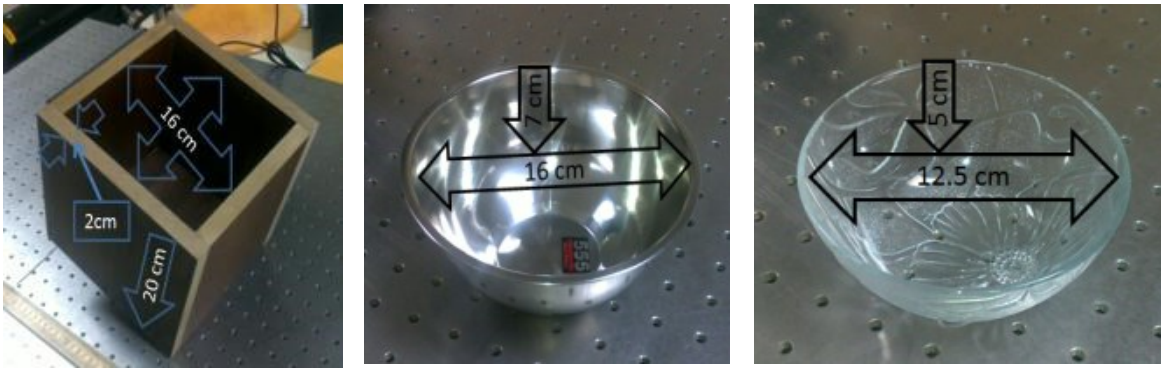

Figure 3.22: Different materials used to cover the tag

In the following sets of figures, the effects of covering the tag located at the center of the room are presented. The point (d4) is chosen at coordinate (0,0,1.43)m as was shown in Figure 3-7. This point has a LOS to all sensors.

Covering the tag with a wood box shifts the mean of the error by almost 20 cm as can be seen in the first plot of where the blue curve corresponds to the case when the tag was at point d4 and not covered and the red curve correspond to the case after the tag is covered.

When the tag is covered by the bowl, the mean of the error is shifted to higher value by almost 40 cm as shown in the same figure.

Covering the tag with steel bowl affects the error range more. The mean of the error is shifted by almost 60 cm as shown in the third plot of Figure 3.23. The individual components are depicted in the fourth part of the figure, most of the error comes from *x* and *y* components.

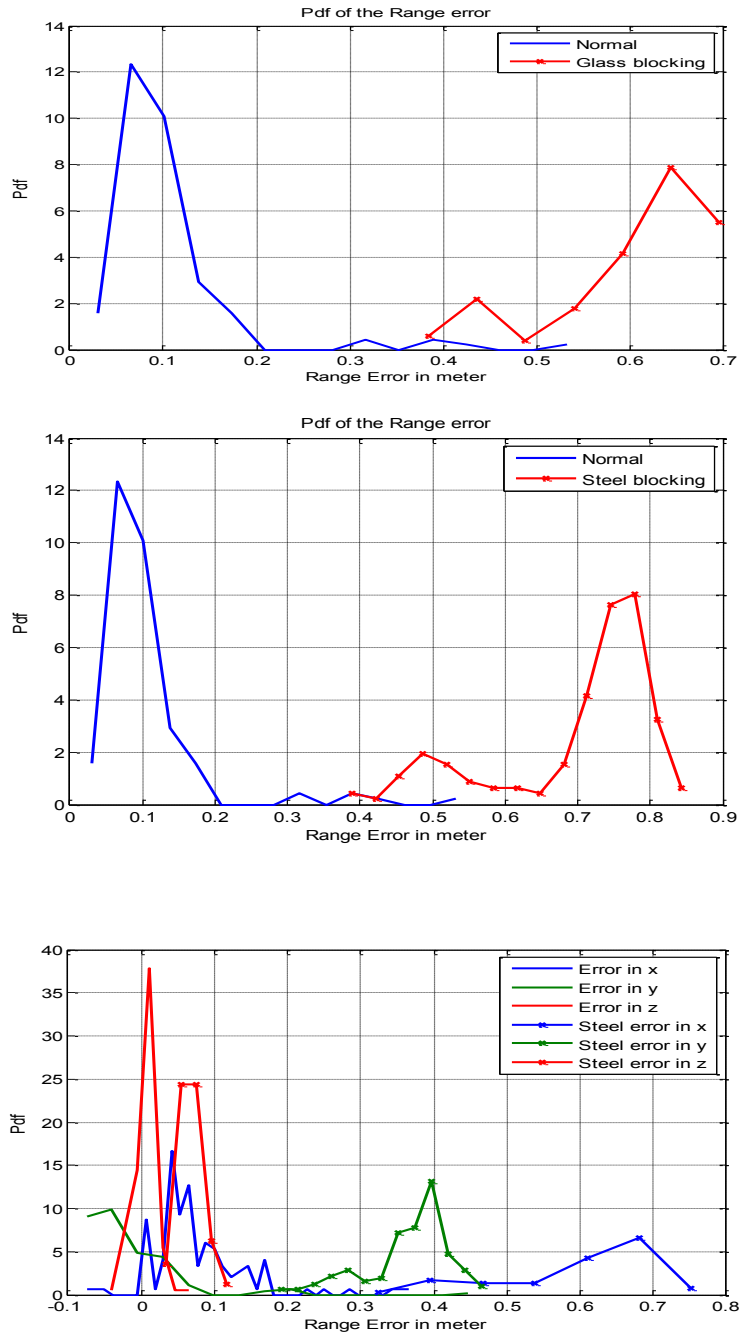

Figure 3.23: The effect of covering the tag with a wooden box (upper), glass bowl (second), steel bowl (lower two)

In this case, the tag is covered by the steel and glass bowl together at the same time. The error is shifted up by about 80 cm (see Figure 3.24). This is due to error in all the components, mainly *x* and *y* components.

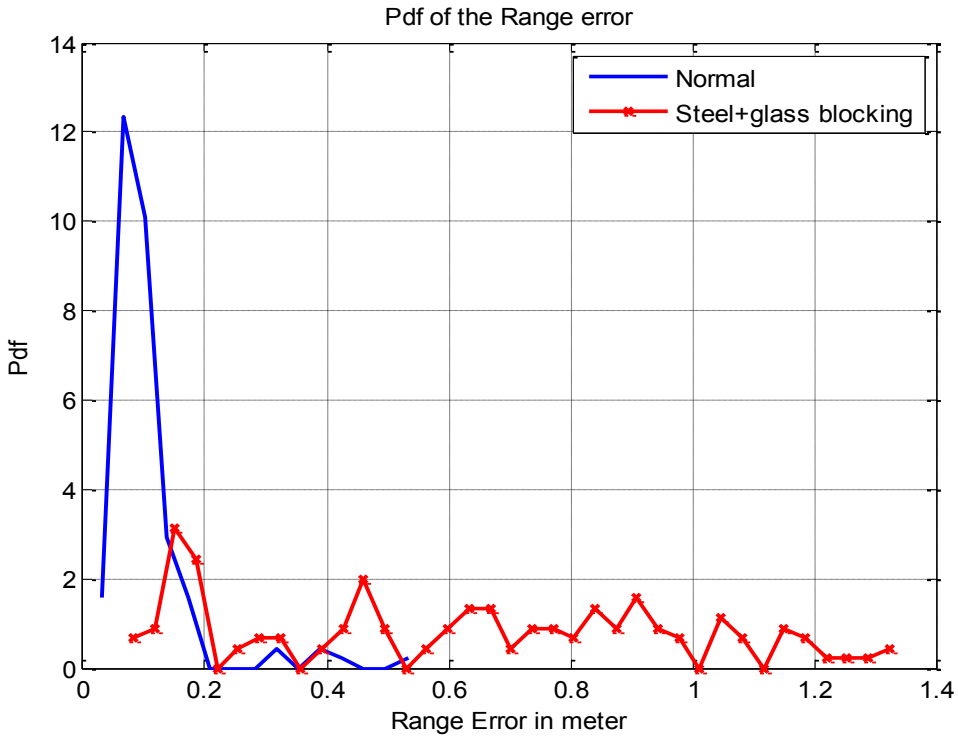

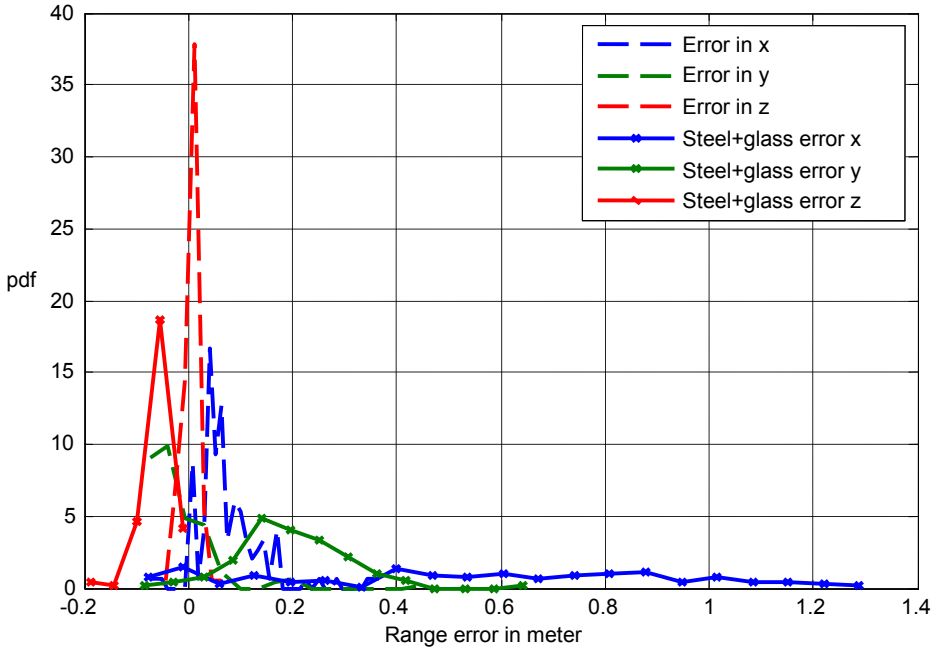

Figure 3.24: The effect of covering the tag with steel and glass bowls

CHAPTER 4 IMPROVED RESIDUAL WEIGHTING ALGORITHM

4.1 Introduction

Wireless localization techniques (UWB based and others) are affected by several sources of errors such as multipath propagation, resulting in fading, or multiple access interference. In addition to the mentioned sources of errors, wireless localization techniques are affected severely by the NLOS propagation that occurs when there is no direct path between the mobile station (MS) and the base station (BS). The effect of NLOS is that it will introduce a positive bias to the range measurement. Therefore, there is a great need to develop algorithms to mitigate the effect of NLOS in order to get a high-resolution range measurement.

In this chapter, an improved residual weighting for TDOA localization algorithms is proposed to mitigate NLOS biases in UWB positioning systems.

4.2 TDOA and the Approximate Maximum Likelihood (AML)

This section will summarize the Approximate Maximum Likelihood (AML) algorithm proposed by Chan [Cha06b]. The Maximum Likelihood (ML) is an optimal algorithm. However, AML is less complex and perform close to ML algorithm and will be used for localization in our work. TDOA localization algorithms use the differences in signal time

of arrivals between a tag and the reference nodes. The vector of TDOA measurements can be represented as

$$T_d = \begin{bmatrix} t_{21} & t_{31} & \cdots \end{bmatrix} \tag{4.1}$$

where t_{N1} represent the time difference of arrival between the N^{th} reference node and the master node, chosen to be S_1, and N represents the number of reference nodes.

$$t_{N1} = t_N - t_1 \tag{4.2}$$

The common reference in these measurements is the time of arrival between the tag and the first reference node. Therefore, there is a correlation between and the vector of TDOA and a covariance matrix given by

$$Q_d = E\left\{T_d T_d^T\right\} \tag{4.3}$$

$$Q_d = \begin{bmatrix} \sigma_2^2 + \sigma_1^2 & \sigma_1^2 & \sigma_1^2 & \cdots & \\ \sigma_1^2 & \sigma_3^2 + \sigma_1^2 & \sigma_1^2 & \cdots & \\ \sigma_1^2 & \sigma_1^2 & \sigma_4^2 + \sigma_1^2 & \cdots & \\ \vdots & \vdots & \vdots & \ddots & \vdots \\ \sigma_1^2 & \sigma_1^2 & \sigma_1^2 & \cdots & \sigma_1^2 \end{bmatrix} \tag{4.4}$$

where σ_i^2 represent the measurement noise variance at the i^{th} reference node. The inverse of this covariance matrix is given by

$$Q_d^{-1} = \text{inv}\left(Q_d\right) \tag{4.5}$$

Now as in [Cha06b] let

$$d_{i1} = r_i - r_1 \tag{4.6}$$

and

$$d = \begin{bmatrix} d_{21} & d_{31} \cdots \end{bmatrix} \tag{4.7}$$

Then, the probability density function of T_d given θ is

$$f\left(T_d|\boldsymbol{\theta}\right) = (2\pi)^{\frac{-(N-1)}{2}} \left(\det \boldsymbol{Q_d}\right)^{\frac{-1}{2}} exp\left\{-\frac{J_d}{2}\right\} \tag{4.8}$$

Where J_d is given by the following relation

$$J_d = \left[\boldsymbol{T}_d - \frac{\mathbf{d}(\theta)}{c}\right]^T \boldsymbol{Q}_d^{-1} \left[\boldsymbol{T}_d - \frac{\mathbf{d}(\theta)}{c}\right] \tag{4.9}$$

, and $\theta = \begin{bmatrix} x & y \end{bmatrix}$ which represents the emitter location.

Setting the gradient of J_d to zero with respect to θ gives the following relation:

$$W\tilde{} \tag{4.10}$$

where

$$\tilde{} \qquad \Delta_{21} \cdots \qquad \Delta_{N1}\Big]^T \tag{4.11}$$

With $\Delta_{21} = ct_{i1}$, and

$$W = \left[\frac{\partial \mathbf{d}(\boldsymbol{\theta})}{\partial \theta}\right]^T Q_d^{-1} \tag{4.12}$$

Now, substituting

$$d_{i1} - \Delta_{i1} = \frac{r_i^2 - (r_1 + \Delta_{i1})^2}{r_i + r_1 + \Delta_{i1}} \tag{4.13}$$

into (4.12) changes it to

$$\mathbf{\Phi} a = 0 \tag{4.14}$$

where

$$\mathbf{\Phi} = W\mathrm{A} \tag{4.15}$$

and

$$\mathrm{A} = diag\left[\frac{1}{r_2 + r_1 + \Delta_{21}} \quad \cdots \quad \frac{1}{r_N + r_1 + \Delta_{N1}}\right] \tag{4.16}$$

and

$$a = \left[r_2^2 - (r_1 + \Delta_{21})^2 \quad \cdots \quad + \Delta_{N1})^2\right]^T \tag{4.17}$$

Now, expanding the elements in a as

$$r_i^2 - (r_1 + \Delta_{i1})^2 = 2(x_1 - x_i)x + 2(y_1 - y_i)y + k_i - k_1 - 2r_1\Delta_{i1} - \Delta_{i1}^2 \tag{4.18}$$

where, $k_i = x_i^2 + y_i^2$ and putting them into (4.17) gives the matrix equation,

$$2\boldsymbol{\Phi D}\theta = \boldsymbol{\Phi}\left(\boldsymbol{\upsilon}_1 + \boldsymbol{r}_1\boldsymbol{\psi}\right) \tag{4.19}$$

where

$$\mathbf{D} = \begin{pmatrix} x_1 - x_2 & y_1 - y_2 \\ \vdots & \vdots \\ x_1 - x_N & y_1 - y_N \end{pmatrix} \tag{4.20}$$

$$\upsilon_1 = \begin{bmatrix} \Delta_{21}^2 + k_1 - k_2 & \cdots & k_1 - k_N \end{bmatrix}^T \tag{4.21}$$

and

$$\psi = 2\begin{bmatrix} \Delta_{21} & \cdots \end{bmatrix} \tag{4.22}$$

Although (4.21) is linear equation in $\boldsymbol{\theta}$, the matrix $\boldsymbol{\Phi}$ contains elements of $\boldsymbol{\theta}$. Therefore, there is a need to use AML to solve for $\boldsymbol{\theta}$. Letting $\boldsymbol{\Phi}$ be an identity matrix in (4.21) simplifies it to

$$2\mathbf{D}\boldsymbol{\theta} = \left(\upsilon_1 + \mathrm{r}_1\psi\right) \tag{4.23}$$

Now, applying weighted LS on (4.23) gives

$$\boldsymbol{\theta} = \frac{1}{2}\left(\mathbf{D}^T Q_d^{-1}\mathbf{D}\right)^{-1}\mathbf{D}^T Q_d^{-1}\left(\upsilon_1 + \mathrm{r}_1\psi\right) \tag{4.24}$$

This solution will give $\boldsymbol{\theta}$ in terms of r_1. Where r_1 represent the true distance between the emitter and the sensor. It is given by,

$$r_1^2 = \left(x - x_1\right)^2 + \left(y - y_1\right)^2 \tag{4.25}$$

Substituting this $\boldsymbol{\theta}$ into (4.25) produces an equation that is quadratic in r_1, and the root selection routine (RSR) will select the best root as follows. If only one root is positive, it is chosen as the best root. If both roots are positive, the routine will choose the one that minimize the cost function J_d. If both roots are negative or imaginary, it takes the absolute value of the real parts.

After selecting the best root the AML takes $\boldsymbol{\theta}$ from this step to calculate $\boldsymbol{\Phi}$, and then from (4.19)

$$\boldsymbol{\theta} = \frac{1}{2}\left(\boldsymbol{\Phi}\mathbf{D}\right)^{-1}\boldsymbol{\Phi}\left(\upsilon_1 + \mathrm{r}_1\psi\right) \qquad (4.26)$$

Again, we have $\boldsymbol{\theta}$ in terms of r_1, and following the procedure after (4.26) gives the updated values of $\boldsymbol{\theta}$**.** Repeating (4.26) with new values of $\boldsymbol{\theta}$ by, say 5 times, produces 5 values of $\boldsymbol{\theta}$ After that, the AML will choose the minimum.

It is important to mention that ML equation of (4.26) is exact, but the solution is approximate because the unknown terms, $\boldsymbol{\theta}$**,** appears in both sides of the equation. The algorithm iteratively updates the values of $\boldsymbol{\theta}$ and other parameters, beginning with the first estimate of $\boldsymbol{\theta}$ from the linear estimator.

4.3 Residual Weighting Algorithm R_{wgh}

This section will summarize the AML algorithm proposed by Chen [Che99]. The main advantage and motive to Chen algorithm is that it is not required to know any prior statistical information about the NLOS channel. The only requirement is to have the minimum needed reference nodes to locate the target (three nodes in 2D localization). The problem of finding the location of a target node can be formulated as an estimation problem. Using Lease Squares (LS) estimator, the location of the target node is given by

$$\hat{x} = \arg\min \sum_{i \epsilon} \left(r_i - x - X_i \right)^2 \tag{4.27}$$

where

S : The reference node index set.

r_i : The range measurement between the target node and the ith reference node.

x : The 2D location of the target node.

$\hat{x}$: The estimate of the vector x .

X_i : The 2D location of the ith reference node.

The effect of the NLOS error will be a bias in the range measurement r_i . The term $\left(r_i - x - X_i \right)$ is referred to as the i^{th} residual for a particular x and is abbreviated as $R_{es}\left(x, S \right)$. It is obvious by referring to equation (4.27) that the LS location solution $\hat{x}$ is

the one that minimizes the total sum of the residual squares for the data set. Equation (4.27) can be re-written as

$$\hat{x} = \arg\min \sum_{i \epsilon} R_{es}(x, S) \tag{4.28}$$

Therefore, the best estimate is the one with the minimum residual. In other words, data sets with NLOS bias will give a large residual and hence a bad location estimate as oppose to the data set without NLOS bias.

The idea behind the residual weighting is to first group the reference nodes into different combinations. After that, the intermediate LS estimate is calculated for each of the different sets along with the normalized residual for each set where the normalized residual is the residual normalized by the number of reference nodes in a particular set. Finally, the final estimate is found as the weighted linear combination of the intermediate estimates for the different sets. The weight is inversely proportional to the normalized residual. In other words, the sets with NLOS bias will have a large normalized residual and hence will be given a less weight (inverse of the residual) as oppose to those sets with small-normalized residuals.

Given *N* reference nodes, the algorithm can be mathematically represented and summarized as the following:

1. We form *M* different sets with each one having at least three reference nodes.

$$M = \sum_{i=3}^{N} \binom{N}{i} \tag{4.29}$$

2. For each combination, we compute the LS estimate (equation (4.28)) and the normalized residuals.

$$\tilde{} = \frac{R_{es}(x, S)}{\text{Size of set } i} \tag{4.30}$$

3. Finally the final estimate is found as linear combination of the weighted intermediate estimates as:

$$\hat{x} = \frac{\sum_{k=1}^{N} \hat{x}_i \tilde{}}{\sum_{k=1}^{N} \tilde{}} \tag{4.31}$$

4.4 Improved Residual Weighting Algorithm for TDOA Techniques

The original Rwgh algorithm is very effective to use with TOA localization techniques for the mitigation of NLOS biases. And this is because TOA localization techniques depends on the intersection of circles and if there is bias in some of the TOA measurements, these circles will not intersect in an exact location which will lead to high residual from this set of measurements. When the Rwgh algorithm is used with TDOA localization techniques it is found that all the sets of three reference nodes will have very small residuals even if some of them have NLOS biases. It is proposed to limit the minimum number of reference nodes to four instead of three. The proposed algorithm gives a good improvement as shown in the simulations section. More explanation of this problem is provided in the following examples.

In Figure 4-1 we show three reference nodes at points (10, 10), (0, 10), and (5, 0) and one tag at location (6, 12), where all of the given coordinates are in meters. If all the sensors are LOS, the two-measured TDOA will give us two hyperbolas H_1 and H_2. The TDOA algorithm will estimate the location of the tag from the intersection of the two hyperbolas. If we assume that there is a bias of 5m in the second reference node (S_2) the TDOA algorithm will estimate the location of the tag from the intersection between the two hyperbolas H_2 and H_3. In this case the estimated location of the tag has a large error and very small residual if the measurement noise is small.

In **Error! Reference source not found.** we show the same sensors with different tag at ocation (6, 9). If all the sensors are LOS, the two-measured TDOA will produce two hyperbolas H_1 and H_2 and the TDOA algorithm will estimate the location of tag from the intersection of the two hyperbolas. Now if we assume that there are two biases of 3 and 4 meters at sensors S_2 and S_3, respectively, then the TDOA algorithm will produce two new hyperbolas H_3 and H_4. From the intersection of the two new hyperbolas, location of the tag will be estimated. With this estimated location, we have a large error and small residual.

When the number of sensor is greater than three and some of the sensor are NLOS then the number of hyperbolas will be more than two. In this situation, the hyperbolas will not intersect at one point and the TDOA algorithm will produce estimates of the location that have high residuals. For this reason, we propose to exclude all the sets of three reference nodes from the R_{wgh} algorithm.

This means that if we are given N reference nodes and the TDOA measurements at these nodes and the TOA measurement at the first reference node, the improved algorithm can be mathematically represented and summarized as follows:

1. We form M different sets with each one having at least four reference nodes.

$$M = \sum_{i=4}^{N} \binom{N}{i} \tag{4.32}$$

2. For each combination we compute the estimated location of the tag using the AML-TDOA algorithm.

3. Use the TDOA measurements, the TOA measurement at the first reference node, and the estimated location for every set to compute the normalized residuals of all the M sets.

$$\tilde{} = \frac{R_{es}(x, S)}{\text{Size of set } i} \tag{4.33}$$

4. Finally the final estimate of the tag location is found as linear combination of the weighted intermediate estimates as:

$$\hat{x} = \frac{\sum_{k=1}^{N} \hat{x}_i \tilde{}^{-1}}{\sum_{k=1}^{N} \tilde{}^{-1}} \tag{4.34}$$

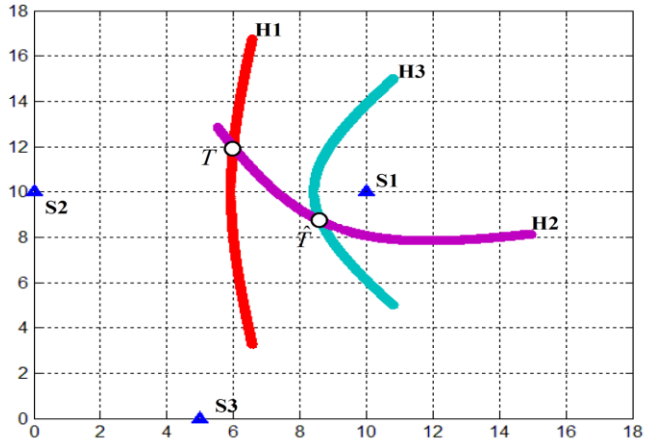

Figure 4-1: Three sensor at at (10, 10), (0, 10), and (5, 0) and one tag at location (6, 12). H1 and H2 are produced from TDOA algorithm if all of the sensors are LOS. H3 is produced if S2 is NLOS

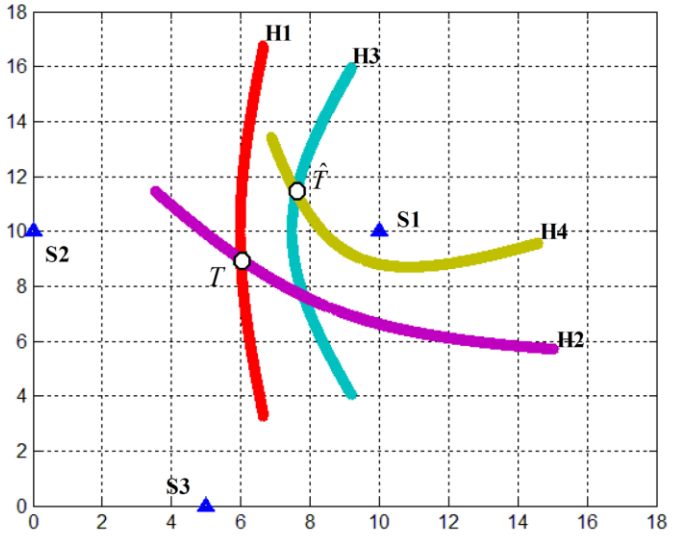

Figure 4-2: Three sensor at (10, 10), (0, 10), and (5, 0) and one tag at location (6, 9). H_1 and H2 are produced from TDOA algorithm if all of the sensors are LOS. H_3 is produced if S_2 is NLOS. H_4 is produced if S3 is NLOS

4.5 System Model

We considered a single cell of radius *R* and *N* reference nodes distributed at the borders of the cell as shown in Figure 4-3. We also assume that we have a tag with unknown location, the possible locations of the tag are assumed to be uniformly distributed in a circle around the center of the cell with radius (R-1), which makes the minimum distance between any possible tag location, and any reference nod is 1 m. For the radio channel between the sensors and the tags, we assume that the tag signal is subject to attenuation including distance path loss and log normal shadowing according to

$$PL(d) = PL_o + 10n\log_{10}\left(\frac{d}{d_o}\right) + \chi, \qquad d \geq d_o \tag{4.35}$$

Where PL_o is the path loss at $d_o = 1$ m, n is the path-loss exponent, and χ is the lognormal shadowing.

For a given tag, shadowing at the different reference nodes is partially correlated, and given by:

$$\chi = a\chi_c + b\chi_i \tag{4.36}$$

where χ_c and χ_i are the common and independent terms, respectively, and $a^2 + b^2 = 1$. In the numerical results, we assume the shadowing variables are lognormal with 50% correlation $(a = b = 0.7071)$. The path-loss exponent and shadowing parameters are according to the IEEE 802.15.4a channel model [Gez05]. IEEE 802.15.4a channel model provides models for UWB channels operating at frequencies in the range of 2 to 10 GHz

that covers indoor residential, indoor office, industrial, outdoor, and open outdoor environments for both LOS and NLOS cases.

In the system model, we assume that the tag has a constant transmitting power and when it is at 1 m from any reference node the signal will is received with a signal to noise ration SNR equal to SNR_o dB. According to the lower bounds on the TOA estimation, we can assume that the variances of the TOA measurements are according to [Bot04], [Gez05b], and [Gez08b]:

$$\sigma_{TOA}^2 = \frac{\kappa}{8\pi SNR\beta^2} \tag{4.37}$$

where κ is a constant greater than one that depends on the accuracy of the TOA estimators and it is assumed to be 1.2 in the simulation section, *SNR* is the signal to noise ratio, and β is the effective bandwidth of the signal between the tag and the reference node.

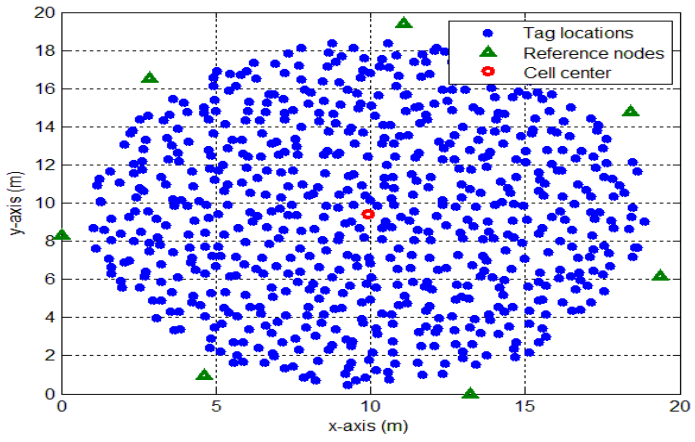

Figure 4-3: Two-dimensional geometry of a cell with seven reference nodes and possible locations of a tag

4.6 Simulations and Discussion of Results

This section summarizes the simulation results based on the improved residual weighting algorithm for TDOA localization techniques. The improvement gained when using the proposed algorithm is examined first. Then, the effect of increasing the signal to noise ratio or the cell size is discussed. Finally, the effects of the changing the number of reference nodes or changing the environment type are investigated.

Figure 4-3 shows the main geometry used to run the simulation. The cell consists of seven reference nodes and the tags in between. The tags locations are uniformly distributed in a circle around the center of the cell with radius equals to *(R-1)*, where *R* is the cell radius. The size of the cell is chosen to be 20m × 20m to comply with the practical cell size in ultra wideband technology. It is to be mentioned that all the units in the figure are in meters.

4.6.1 Comparing the Improved R_{wgh} algorithm with original R_{wgh} algorithm

This part discusses the improvement gained with the proposed algorithm. The number of reference nodes used in this simulation is eight and the SNR is 30 dB at a location of one meter from the reference node. The coordinates for the eight reference nodes are summarized in Table 4-1. Referring to the IEEE 802.15.4a channel model, the environment type for this simulation is indoor office where the values of the standard deviation of the shadowing and the pathloss exponent are given in Table 4-2.

	1	2	3	4	5	6	7	8
x-coordinate (m)	11.280	17.881	19.810	15.937	8.531	1.929	0	3.873
y-coordinate (m)	0	3.873	11.280	17.881	19.810	15.937	8.531	1.929

Table 4-1: Geometry of the eight reference nodes

	Path-loss exponent (n)	Standard deviation for Shadowing (σ_{sh})
LOS	1.63	1.9
NLOS	3.07	3.9

Table 4-2: Path-loss parameters for indoor office environment

In the case of a single bias, the chosen reference node is S_2 and the added bias is uniformly distributed between zero and the maximum bias, where the maximum bias is 100% of the real distance between the tag and the reference node. In Figure 4-4, the x-axis is the maximum bias and the y-axis represents the average location error. Figure 4-4 shows a good improvement in the mitigation of NLOS biases when the proposed algorithm is used compared to the original Rwgh-TDOA algorithm by Chen. The same figure, also, shows a good improvement to mitigate two and three NLOS biases. The two biases are with S2 and S3 and the three biases are with S2, S3, and S4. It is clear from the figure that we have better localization in the case of one bias than the case of two and

three biases. The improvement of the proposed algorithm compared with Chen algorithm is expected even with increasing the number of NLOS biases as far as the number of reference nodes that has a direct path (LOS) to the tag is more than three.

It can be also noticed that the average location error decreases with the increase in the ratio of the maximum bias. The reason is that an increase in the ratio of the bias will result in an increase in the residual of the NLOS sets and hence the given weight that is the reciprocal of the residual will be less for those sets. Therefore, there will be an improvement in the Rwgh final estimate and hence a reduction in the average location error.

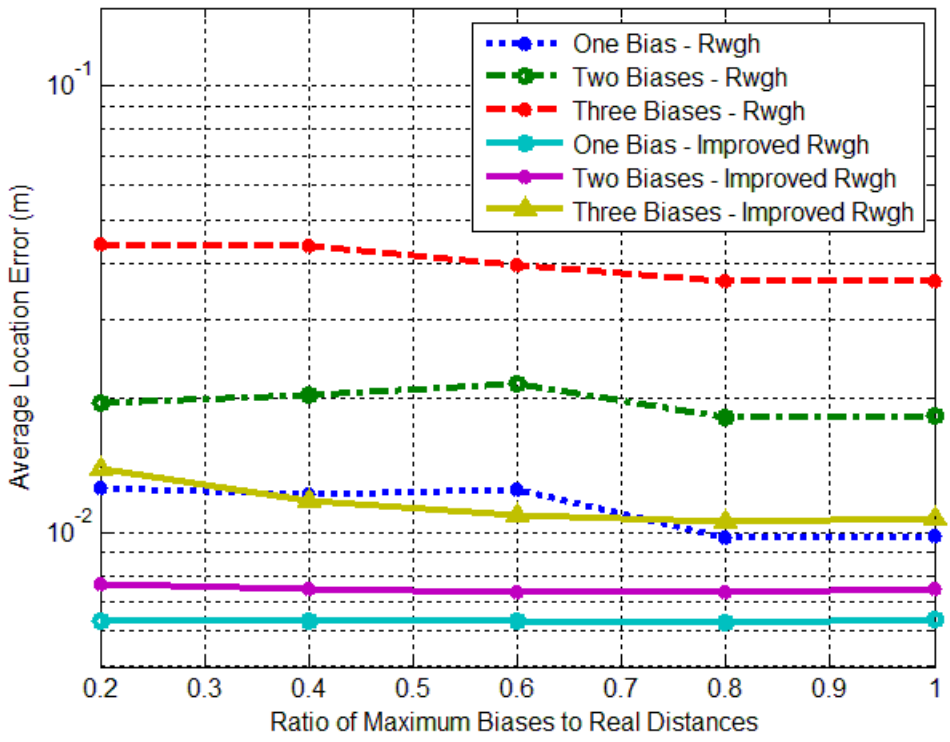

Figure 4-4: Comparing the proposed algorithm with the original Rwgh algorithm in mitigating one, two, and three NLOS biases

4.6.2 The effect of increasing the signal to noise ratio on the accuracy of the algorithm

In this part, the effect of changing the SNR at a distance of one meter from the reference nodes is investigated. The SNR is varied between 10 dB and 50 dB in a step of 10 dB. Seven reference nodes are used in this simulation and their geometry locations are summarized in Table 4.3. Two NLOS biases are assumed in the TOA measurements at the reference nodes S2 and S3. In addition, the indoor office environment is assumed in this simulation with the exactly the same parameter in Table 4-2 above. The simulation result shows that the average error in the localization of the tag decreases when increasing the SNR. One possible reason is that increasing the SNR will decrease in the noise variances at the reference nodes. The details of the results are shown in Figure 4-5 below.

In addition, the average location error decreases with the increase in the ratio of the maximum bias for the different SNR values. The reason is that an increase in the ratio of the bias will result in an increase in the residual of the NLOS sets and hence the given weight which the reciprocal of the residual will be less for those sets. Therefore, there will be an improvement in the Rwgh final estimate and hence a reduction in the average location error.

	1	2	3	4	5	6	7
x-coordinate (m)	13.240	19.376	18.404	11.057	2.866	0	4.617
y-coordinate (m)	0	6.136	14.759	19.376	16.510	8.319	0.972

Table 4.3: Geometry of the seven reference nodes

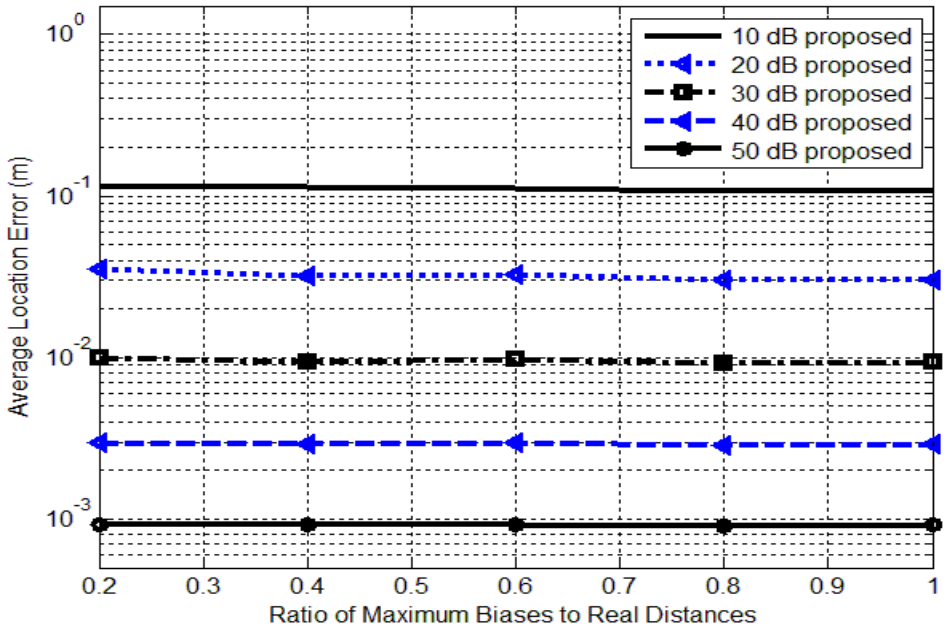

Figure 4-5: The effect of increasing the SNR

4.6.3 The effect of the cell size on the accuracy of the algorithm

In this part the effect of changing the radius of the cell on the accuracy of the algorithm is investigated. The SNR is assumed to be 30 dB at 1 m from the reference nodes. The geometry of Figure 4-3 is used in this simulation with the biases at S_2 and S_3. In addition, the indoor office environment is assumed in this simulation with the exactly the same parameter in Table 4-2 above. The simulation result shows that the average error in the tag locations increases when the cell size increases. One possible reason is that increasing the cell radius will result in an increase in the noise variance at the reference nodes. The details of the results are shown in Figure 4-6 below.

It can be also noticed that the average location error decreases or increase with the increase in the ratio of the maximum bias for the different cases of the cell radius. The possible reason is due to the different realization of the added noise for the different values of the bias.

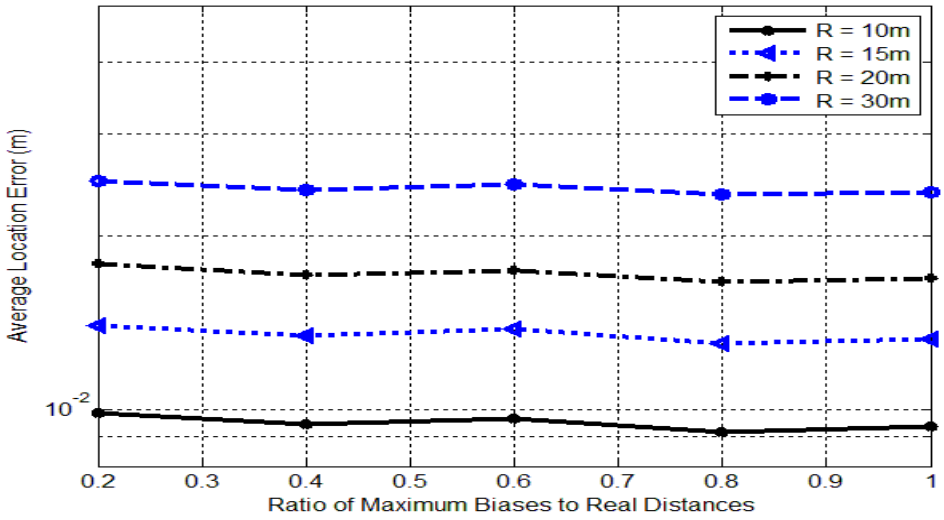

Figure 4-6: The effect of changing the radius of the cell

4.6.4 The effect of the number of sensors on the accuracy of the algorithm

In this part, the effect of changing the number of reference nodes in the cell is discussed. The results are for the cases when the number of reference nodes in the cell is 6, 7 or 8. In the case of six reference nodes, the locations of the nodes are summarized in Table 4.4. Similar to the other simulations, the tags locations are uniformly distributed in a circle around the center of the cell with radius equals to (*R*-1), where *R* is the cell radius. It is assumed that the SNR is 30 dB at 1 meter form the reference nodes. In addition, the indoor office environment is simulated with S_2 and S_3 under NLOS conditions. The obtained results show (see Figure 4-7) that increasing the number of reference nodes in the cell will improve the performance of the localization algorithm.

As previously discussed, the idea of the R_{wgh} is based on forming different sets with each one having 4 different nodes. Therefore, it is obvious that increasing the number of nodes will result in increasing the number of sets and hence a better location estimation.

In addition, it can be noticed that the value of the average location error increases or decreases with the increase of the ration of the maximum biases. This is mainly due to the different realization of the added noise at the different values of the bias.

	1	2	3	4	5	6
x-coordinate (m)	7.071	16.730	19.319	12.247	2.588	0
y-coordinate (m)	0	2.588	12.247	19.319	16.730	7.071

Table 4.4: Geometry of the six reference nodes

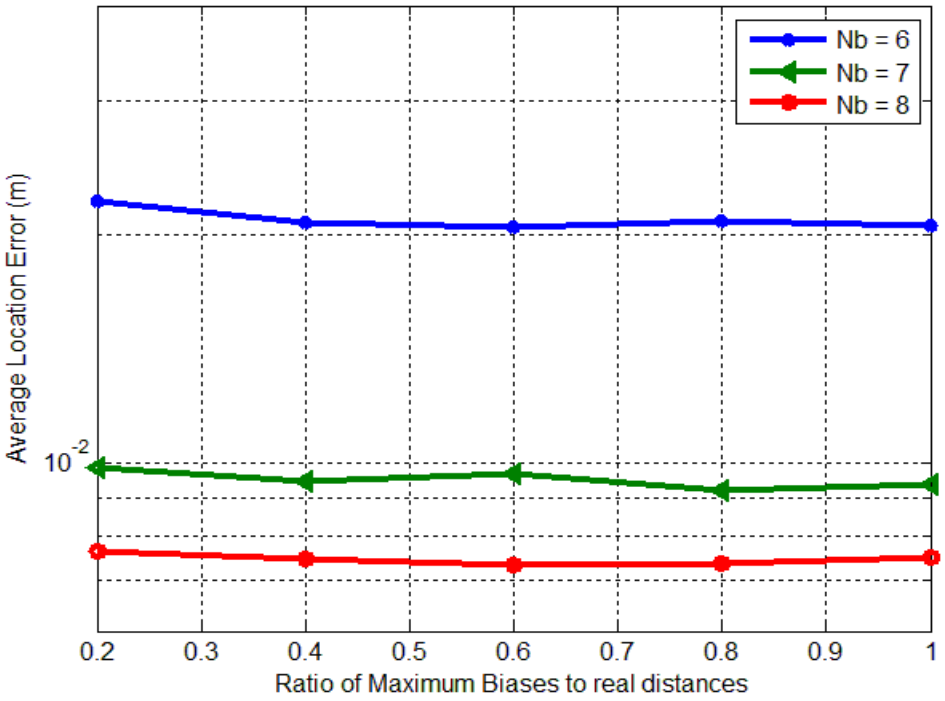

Figure 4-7: The effect of changing the number of sensors

4.6.5 The performance of the algorithm under different environment

In this part, the performance of the proposed algorithm with different environments is discussed. Three different environments are simulated and the detailed parameters of these environments are obtained for the IEEE 802.15.4a channel model as shown in the Table 4.5 below.

Environment Type	Path-loss exponent (n)		Standard deviation for Shadowing (σ_{sh})	
	LOS	NLOS	LOS	NLOS
Indoor office	1.63	3.07	1.9	3.9
Outdoor office	1.76	2.5	0.83	2
Industrial	1.2	2.15	6	6

Table 4.5: Path-loss parameters for IEEE 802.15.4a channel model

The SNR is fixed to a value of 30 dB at 1 m from the reference nodes for the different environments. The geometry of Figure 4-3 is used in this simulation with the bias at S_2 and S_3. Figure 4-8 show that the industrial environment gives the least average location error when compared with the other two environments. The reason is that the pathloss exponent in the industrial environment is the least as can be concluded from Table 4-2. Less pathloss exponent will result in a less pathloss and hence a larger received SNR and smaller error variance.

In addition, for the different types of the environment, the average location error increases or decreases with the increase of the ration of the maximum biases. This is mainly due to the different realization of the added noise at the different values of the bias.

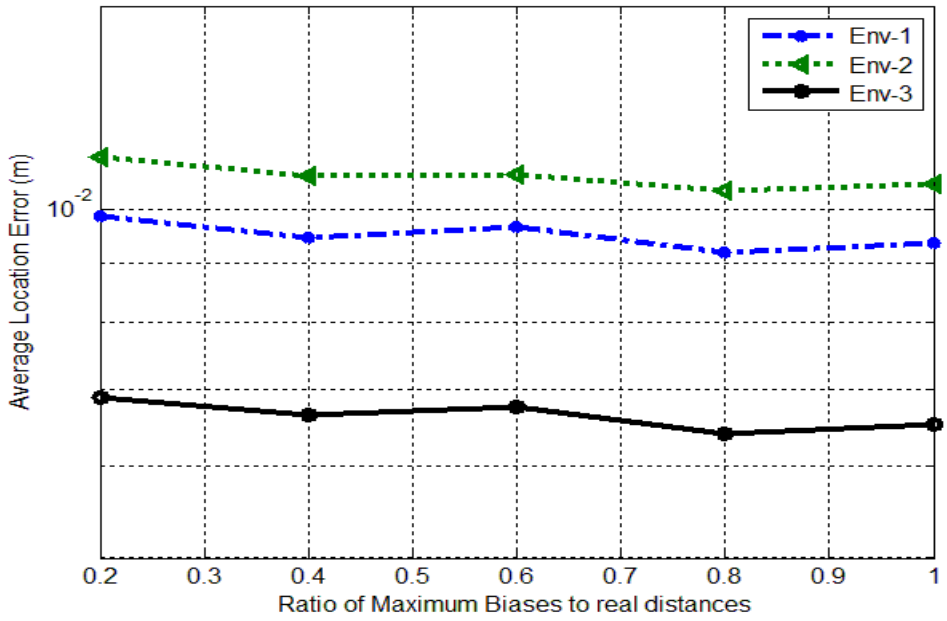

Figure 4-8: The performance of the algorithm with different environment

4.7 Conclusion

In this chapter, a residual weighting algorithm (R_{wgh}) is used to mitigate the effect of NLOS bias. The algorithm does not require any prior statistical information about the NLOS channel. The principle is that after grouping the sensors into different sets with each set containing a minimum of three sensors, LS estimate and the normalized residual are calculated for the sets. Finally, the final estimate is found as the weighted linear combination of the intermediate estimates for the different sets. The weight is inversely proportional to the normalized residual. Therefore, sets with NLOS bias will have a large normalized residual and will be given a less weight while sets with no NLOS will have a small-normalized residual and will be given a large weight.

An improved residual algorithm for TDOA techniques is proposed. Chen compares the performance of the proposed algorithm with the original residual weighting algorithm. The simulation results show good improvement over the original algorithm in all the scenarios discussed in the chapter.

CHAPTER 5 CONCLUSIONS AND RECOMMENDATIONS

5.1 Summary and Conclusions

5.2 Recommendation for Future Research

References

[Ala06a] B. Alavi, K. Pahlavan, ”**Modeling of TOA-based distance measurement error using UWB indoor radio measurements**”, IEEE Communication Letters, vol. 10, no. 4, pp. 275-277, Apr. 2006.

[Bot04] C. Botteron, A. Host-Madsen, and M. Fattouche, BCramer–Rao “**bounds for the estimation of multipath parameters and mobiles’** positions in asynchronous DS-CDMA systems, IEEE Trans. Signal Process., vol. 52, pp. 862–875, Apr. 2004.

[Caf98] J. J. Caffery and G. L. Stuber, “**Overview of radiolocation in CDMA cellular systems,**” *IEEE Commun. Mag.*, vol. 36, no. 4, pp. 38–45, Apr. 1998.

[Cas06] R. Casas, A. Marco, J. J. Guerrero, and J. Falco, “**Robust estimator for non-line-of-sight error mitigation in indoor localization**,” *EURASIP Journal on Applied Signal Processing*, vol. 2006, pp. Article ID 43 429, 8 pages, 2006, doi:10.1155/ASP/2006/43429.

[Cha06a] Y. T. Chan, C. H. Yau, and P. C. Ching "**Time-of-Arrival Based Localization under NLOS Conditions**" *IEEE Trans. Veh*, vol.55, no.1, 2006, pp.17- 24.

[Cha06b] Y. T. Chan, C. H. Yau, and P. C. Ching, “**Exact and approximate maximum likelihood localization algorithms,**” *IEEE Trans. Veh. Technol,* vol. 55, no1, pp. 10-16, Jan 2006.

[Che99] P. C. Chen, "**A non-line-of-sight error mitigation algorithm in location estimation**," in *Proc. IEEE Int. Conf. Wireless Commun. Networking (WCNC)*, vol. 1, New Orleans, LA, Sep. 1999, pp. 316–320.

[End11] Enda, K.; Kohno, R.; , "**High accuracy TOA positioning algorithm using UWB under NLOS environment for medical network**," *Medical Information & Communication Technology (ISMICT), 2011 5th International Symposium on* , vol., no., pp.79-83, 27-30 March 2011

[Gez05a] S. Gezici, Z. Sahinoglu, H. Kobayashi, H. V. Poor, and A. F. Molisch, "**A two-step time of arrival estimation algorithm for impulse radio ultrawideband systems**," in Proc. 13th European Signal Processing Conference (EUSIPCO), Antalya, Turkey, Sep. 2005.

[Gez05b] S. Gezici, Z. Tian, G. B. Giannakis, H. Kobayashi, A.F. Molisch, H. V. Poor,and Z. Sahinoglu, "**Localization via ultra-wideband radios: A look at positioning aspects for future sensor networks**," *IEEE Signal Processing Mag.*, vol. 22, no. 4, pp. 70–84, July 2005.

[Lee02] J.-Y. Lee and R. A. Scholtz, "**Ranging in a dense multipath environment using an UWB radio link**," *IEEE J. Select. Areas Commun.*, vol. 20, no. 9, pp. 1677–1683, Dec. 2002

[Guv07] Guvenc, I.; Chia-Chin Chong; Watanabe, F.; , "**NLOS Identification and Mitigation for UWB Localization Systems**," *Wireless Communications and Networking Conference, 2007.WCNC 2007. IEEE* , vol., no., pp.1571-1576, 11-15 March 2007.

[Guv05] I. Guvenc and Z. Sahinoglu, "**Threshold-based TOA estimation for impulse radio UWB systems**," in *in Proc. IEEE Int. Conf. UWB (ICU)*, Zurich, Switzerland, Sep. 2005, pp. 420–425.

[Gez08] S. Gezici, **"A survey on wireless position estimation,"** *Wireless Personal Communications*, vol. 44, no. 3, pp. 263–282, Feb. 2008.

[Gus05] F. Gustafsson and F. Gunnarsson, "**Mobile positioning using wireless networks**," *IEEE Signal Processing Mag.*, vol. 22, no. 4, pp.41–53, July 2005.

[Gez05b] S. Gezici, Z. Tian, G. B. Giannakis, H. Kobayashi, A. F. Molisch, H. V. Poor, and Z. Sahinoglu, B **Localization via ultra-wideband adios: A look at positioning aspects for future sensor networks**, IEEE Signal Process. Mag., vol. 22, pp. 70–84, Jul. 2005.

[Gez08b] Gezici, S.; Guvenc, I.; Sahinoglu, Z.; , "**On the Performance of Linear Least-Squares Estimation in Wireless Positioning Systems**," Communications, 2008. ICC '08. IEEE International Conference on , vol., no., pp.4203-4208, 19-23 May 2008.

[Gez09] Gezici, S.; Poor, H.V.; , "**Position Estimation via Ultra-Wide-Band Signals**," *Proceedings of the IEEE* , vol.97, no.2, pp.386-403, Feb. 2009 [Fcc02] Federal Communications Commission, "**First Report and Order 02-48**," Feb. 2002.

[Jia07] Lei Jiao; Jianping Xing; Xuan Zhang; Chaoli Zhao; Jun Zhang; , "**LCC-Rwgh: A NLOS Error Mitigation Algorithm for Localization in Wireless Sensor Network**," *Control and Automation, 2007. ICCA 2007. IEEE International Conference on* , vol., no., pp.1354-1359, May 30 2007-June 1 2007.

[Li06] Fan Li; Wenwu Xie; Jun Wang; Shouyin Liu; , "**A New Two-Step Ranging Algorithm in NLOS Environment for UWB Systems**," *Communications, 2006. APCC '06. Asia-Pacific Conference on* , vol., no., pp.1-5, Aug. 2006.

[Mar10] Maranò, S.; Gifford, W.M.; Wymeersch, H.; Win, M.Z.; , **"NLOS identification and mitigation for localization based on UWB experimental data**," *Selected Areas in Communications, IEEE Journal on* , vol.28, no.7, pp.1026-1035, September 2010

[Kan11] Moon-kyoung Kang; Jimyng Kang; Soon Woo Lee; Young-Jin Park; Kwan-Ho Kim; , "**NLOS mitigation for low-cost IR-UWB RTLS,"** *Ultra-Wideband (ICUWB), 2011 IEEE International Conference on* , vol., no., pp.96-100, 14-16 Sept. 2011

[Yan05] L. Yang and G. B. Giannakis, "**Timing ultra-wideband signals with dirty templates,**" *IEEE Trans. Commun.*, vol. 53, no. 11, pp. 1952–1963, Nov. 2005

[Hei07] Heidari, M.; Akgul, F.O.; Pahlavan, K.; , "**Identification of the Absence of Direct Path in Indoor Localization Systems,**" *Personal, Indoor and Mobile Radio Communications, 2007. PIMRC 2007. IEEE 18th International Symposium on* , vol., no., pp.1-6, 3-7 Sept. 2007.

[IEE06] IEEE P802.15.4a/D4 (Amendment of IEEE Std 802.15.4), "**Part 15.4: Wireless medium access control (MAC) and physical layer (PHY) specifications for low-rate wireless personal area networks (LRWPANs)**," July 2006.

[Sah08] Z. Sahinoglu, S. Gezici, and I. Guvenc, ***Ultra-Wideband Positioning Systems: Theoretical Limits, Ranging Algorithms, and Protocols***.Cambridge University Press, 2008.

[Sah06] Z. Sahinoglu and I. Guvenc, "**Multiuser interference mitigation in noncoherent UWB ranging via nonlinear filtering**," *EURASIP Journal on Wireless Communications and Networking*, vol. 2006, pp. Article ID 56 849, 10 pages, 2006.

[Shi03] Y. Shimizu and Y. Sanada, "**Accuracy of relative distance measurement with ultra wideband system**," in *Proc. IEEE Conf. Ultra Wideband Syst. Technol. (UWBST)*, Reston, VA, Nov. 2003, pp. 374–378.

[Sha07] Shaohua Wu; Yongkui Ma; Qinyu Zhang; Naitong Zhang; , "**NLOS Error Mitigation for UWB Ranging in Dense Multipath Environments**," *Wireless Communications and Networking Conference, 2007.WCNC 2007. IEEE* , vol., no., pp.1565-1570, 11-15 March 2007

[Ven07] Venkatesh, S.; Buehrer, R.M.; , "**NLOS Mitigation Using Linear Programming in Ultrawideband Location-Aware Networks**," *Vehicular Technology, IEEE Transactions on* , vol.56, no.5, pp.3182-3198, Sept. 2007.

[Xu11] Xu, J.; Ma, M.; Law, C.L.; , "**Performance of time-difference-of-arrival ultra wideband indoor localisation,**" *Science, Measurement & Technology, IET* , vol.5, no.2, pp.46-53, March 2011

[Yan05] L. Yang and G. B. Giannakis, "**Timing ultra-wideband signals with dirty templates,**" *IEEE Trans. Commun.*, vol. 53, no. 11, pp.1952–1963, Nov. 2005.

[Yu07] Kegen Yu; Guo, Y.J.; , "**NLOS Error Mitigation for Mobile Location Estimation in Wireless Networks,**" *Vehicular Technology Conference, 2007. VTC2007-Spring. IEEE 65th* , vol., no., pp.1071-1075, 22-25 April 2007.

[Wei04] A. J. Weiss, "**Direct position determination of narrowband radio frequency transmitters**," *IEEE Signal Processing Lett.*, vol. 11, no. 5, pp. 513–516, May 2004.

[Qi06] Y. Qi, H. Kobayashi, and H. Suda, "**Analysis of wireless geolocation in a non-line-of-sight environment**," *IEEE Trans. Wireless Commun.*, vol. 5, no. 3, pp. 672–681, Mar. 2006.

Vita

- Khaled Mesfer AlQahtani
- Born in Riyadh
- Received B.S.c degree in Electrical Engineering from KFUPM, Saudi Arabia in June 2008.
- Completed M.S.c degree requirements at KFUPM, Saudi Arabia in December 2011